

Consequences of natural perturbations in the human plasma proteome

Benjamin B. Sun^{1*}, Joseph C. Maranhville^{2*}, James E. Peters^{1,3*}, David Stacey¹, James R. Staley¹, James Blackshaw¹, Stephen Burgess^{1,4}, Tao Jiang¹, Ellie Paige^{1,5}, Praveen Surendran¹, Clare Oliver-Williams^{1,6}, Mihir A. Kamat¹, Bram P. Prins¹, Sheri K. Wilcox⁷, Erik S. Zimmerman⁷, An Chi², Narinder Bansal^{1,8}, Sarah L. Spain⁹, Angela M. Wood¹, Nicholas W. Morrell¹⁰, John R. Bradley¹¹, Nebojsa Janjic⁷, David J. Roberts^{12,13}, Willem H. Ouwehand^{3,14,15,16,17}, John A. Todd¹⁸, Nicole Soranzo^{3,14,16,17}, Karsten Suhre¹⁹, Dirk S. Paul¹, Caroline S. Fox², Robert M. Plenge², John Danesh^{1,3,16,17}, Heiko Runz^{2*}, Adam S. Butterworth^{1,17*}

1. MRC/BHF Cardiovascular Epidemiology Unit, Department of Public Health and Primary Care, University of Cambridge, Cambridge CB1 8RN, UK.
2. MRL, Merck & Co., Inc., Kenilworth, New Jersey, USA.
3. British Heart Foundation Cambridge Centre of Excellence, Division of Cardiovascular Medicine, Addenbrooke's Hospital, Cambridge CB2 0QQ, UK.
4. MRC Biostatistics Unit, University of Cambridge, Cambridge CB2 0SR, UK.
5. National Centre for Epidemiology and Population Health, The Australian National University, Canberra, ACT, Australia.
6. Homerton College, Cambridge, CB2 8PH, UK.
7. SomaLogic Inc., Boulder, Colorado 80301, USA.
8. Perinatal Institute, Birmingham B15 3BU, UK.
9. Wellcome Trust Sanger Institute, Wellcome Trust Genome Campus, Hinxton, Cambridge CB10 1RQ, UK.
10. Division of Respiratory Medicine, Department of Medicine, University of Cambridge, Cambridge CB2 0QQ, UK.
11. NIHR Cambridge Biomedical Research Centre / BioResource, Cambridge University Hospitals, Cambridge CB2 0QQ, UK.
12. National Health Service (NHS) Blood and Transplant and Radcliffe Department of Medicine, NIHR Oxford Biomedical Research Centre, University of Oxford, John Radcliffe Hospital, Oxford OX3 9DU, UK.
13. BRC Haematology Theme and Department of Haematology, Churchill Hospital, Oxford OX3 7LE, UK.
14. Department of Haematology, University of Cambridge, Cambridge Biomedical Campus, Long Road, Cambridge CB2 0PT, UK.
15. National Health Service (NHS) Blood and Transplant, Cambridge Biomedical Campus, Cambridge CB2 0PT, UK.
16. Department of Human Genetics, Wellcome Trust Sanger Institute, Wellcome Trust Genome Campus, Hinxton, Cambridge CB10 1RQ, UK.
17. NIHR Blood and Transplant Research Unit in Donor Health and Genomics, Department of Public Health and Primary Care, University of Cambridge, Cambridge CB1 8RN, UK.
18. JDRF/Wellcome Trust Diabetes and Inflammation Laboratory, Wellcome Trust Centre for Human Genetics, Nuffield Department of Medicine, NIHR Oxford Biomedical Research Centre, University of Oxford, Oxford OX3 7BN, UK.
19. Department of Physiology and Biophysics, Weill Cornell Medicine - Qatar, PO 24144 Doha, Qatar.

* These authors contributed equally to this work.

Corresponding authors: asb38@medschl.cam.ac.uk (A.S.B.), jd292@medschl.cam.ac.uk (J.D.)

50 **Summary** (135 words)

51 Although proteins are the primary functional units of biology and the direct targets of most
52 drugs, there is limited knowledge of the genetic factors determining inter-individual variation
53 in protein levels. Here we reveal the genetic architecture of the human plasma proteome. We
54 identify 1,927 genetic associations with 1,478 proteins, a 4-fold increase on existing
55 knowledge, including *trans* associations for 1,104 proteins. To understand consequences of
56 perturbations in plasma protein levels, we apply an integrated approach that links genetic
57 variation with biological pathway, disease, and drug databases. We provide insights into
58 pathobiology by uncovering the molecular effects of disease-associated variants and
59 identifying causal roles for protein biomarkers in disease through Mendelian randomisation
60 analysis. Our results reveal new drug targets, opportunities for matching existing drugs with
61 new disease indications, and potential safety concerns for drugs under development.

62 (main text: 2,960 words)

63 Plasma proteins play key roles in a variety of biological processes including signalling,
64 transport, growth, repair, and defence against infection. They are frequently dysregulated in
65 disease and are important drug targets. Identifying factors that determine inter-individual
66 protein variability should, therefore, furnish biological and medical insights¹. Despite evidence
67 of the heritability of plasma protein abundance², however, systematic assessment of how
68 genetic variation influences plasma protein levels has been limited^{1,3-5}. Studies have examined
69 intracellular ‘protein quantitative trait loci’ (pQTLs)⁶⁻⁸, but they have tended to be small and
70 used cell lines rather than primary human tissues.

71

72 Here we create and interrogate a genetic atlas of the human plasma proteome, using a markedly
73 expanded version of an aptamer-based multiplex protein assay (SOMAscan)⁹ to quantify 3,622
74 plasma proteins in 3,301 healthy individuals. We identify 1,927 genotype-protein associations,
75 including *trans*-associated loci for 1,104 proteins, providing new understanding of the genetic
76 control of protein regulation. 88 pQTLs overlap with disease susceptibility loci, elucidating the
77 molecular effects of disease-associated variants. Using the principle of Mendelian
78 randomisation¹⁰, we find evidence to support causal roles in disease for several protein
79 pathways, and cross-reference our data with disease and drug databases to highlight novel
80 potential therapeutic targets.

81

82 **RESULTS**

83 **Genetic architecture of the plasma proteome**

84 After stringent quality control, we performed genome-wide testing of 10.6 million imputed
85 autosomal variants against levels of 2,994 plasma proteins in 3,301 healthy European-ancestry
86 individuals (Methods, Extended Data Figure 1). We demonstrated robustness of protein

87 measurements in several ways (Methods, Supplementary Note), including: highly consistent
88 measurements in replicate samples; temporal consistency in protein levels in individuals at
89 timepoints two years apart (Extended Data Figure 2b); replication of known associations with
90 non-genetic factors (Supplementary Tables 1-2). To assess potential off-target cross-reactivity,
91 we tested 920 SOMAmers for detection of proteins with $\geq 40\%$ sequence homology to the target
92 protein (Methods). Although 126 (14%) SOMAmers showed comparable binding with a
93 homologous protein (Supplementary Table 3), nearly half of these were binding to alternative
94 forms of the same protein.

95

96 We found 1,927 genome-wide significant ($p < 1.5 \times 10^{-11}$) associations between 1,478 proteins
97 and 764 genomic regions (Figure 1a, Supplementary Table 4, Supplementary Video 1), with
98 89% of pQTLs previously unreported. Of the 764 associated regions, 502 (66%) had local-
99 acting ('*cis*') associations only, 228 (30%) *trans* associations only, and 34 (4%) both *cis* and
100 *trans* (Supplementary Note Table 1). 95% and 87% of *cis* pQTL variants were located within
101 200Kb and 100Kb, respectively, of the relevant gene's canonical transcription start site (TSS)
102 (Figure 1b), and 44% were within the gene itself. The *p*-values for *cis* pQTL associations
103 increased with distance from the TSS, mirroring findings for expression QTLs (eQTLs)^{11,12}.
104 Of the proteins for which we identified a pQTL, 88% had either *cis* (n=374) or *trans* (n=925)
105 associations only, while 12% (n=179) had both (Supplementary Note Table 1). The majority
106 of significantly associated proteins (75%; n=1,113) had a single pQTL, while 20% had two and
107 5% had >2 (Figure 1c). To detect multiple independent signals at the same locus we used
108 stepwise conditional analysis, identifying 2,658 conditionally significant associations
109 (Supplementary Table 5). Of the 1,927 locus-protein associations, 414 (21%) had multiple
110 conditionally significant signals (Figure 1d), of which 255 were *cis*.

111

112 We were able to test replication of 163 pQTLs in 4,998 individuals using an alternative protein
113 assay (Olink, [Methods](#))¹³. Effect-size estimates for these 163 pQTLs were strongly correlated
114 between the SOMAscan and Olink platforms ($r=0.83$; [Extended Data Figure 2c](#)). 106/163
115 (65% overall; 81% *cis*, 52% *trans*) pQTLs replicated after Bonferroni correction
116 ([Supplementary Tables 4,6](#)). The lower replication rate of *trans* signals may reflect various
117 factors, including differences between protein assays (e.g., detection of free versus complexed
118 proteins) and the higher ‘biological prior’ for *cis* associations.

119

120 Of 1,927 pQTLs, 549 (28.5%) were *cis*-acting ([Supplementary Table 4](#)). Genetic variants that
121 change protein structure may result in apparent pQTLs due to altered aptamer-binding rather
122 than true quantitative differences in protein levels. However, we found evidence against the
123 possibility of such artefactual associations for 371 (67.6%) *cis* pQTLs ([Methods](#),
124 [Supplementary Tables 4, 7-8](#)). Results were materially unchanged when we repeated
125 downstream analyses excluding those *cis* pQTLs without evidence against binding effects.

126

127 The median variation in protein levels explained by pQTLs was 5.8% (in-sample estimate;
128 interquartile range: 2.6-12.4%, [Figure 1e](#)). For 193 proteins, however, genetic variants
129 explained >20% of the variation. There was a strong inverse relationship between effect-size
130 and minor allele frequency (MAF) ([Figure 1f](#)), consistent with previous genome-wide
131 association studies (GWAS) of quantitative traits^{8,14-15}. We found 23 and 208 associations with
132 rare (MAF <1%) variants and low-frequency (MAF 1-5%) variants, respectively
133 ([Supplementary Table 4](#)). Of the 36 strongest pQTLs (per-allele effect-size >1.5 standard
134 deviations), 29 were rare or low-frequency variants.

135

136 Both *cis* and *trans* pQTLs were strongly enriched for missense variants ($p < 0.0001$) and for
137 location in 3' untranslated ($p = 0.0025$) or splice sites ($p = 0.0004$) ([Figure 1g](#), [Extended Data](#)
138 [Figure 3a](#)). We found ≥ 3 -fold enrichment ($p < 5 \times 10^{-5}$) of pQTLs at features indicative of
139 transcriptional activation in blood cells (unsurprisingly given our use of plasma) and at
140 hepatocyte regulatory elements, consistent with the liver's role in protein synthesis and
141 secretion ([Methods](#), [Extended Data Figure 4](#), [Supplementary Table 9](#)).

142

143 **Overlap of eQTLs and pQTLs**

144 An important question is the extent to which genetic associations with plasma protein levels
145 are driven by effects at the transcription level, rather than other mechanisms, such as altered
146 protein clearance or secretion. We therefore cross-referenced our *cis* pQTLs with previous
147 eQTL studies ([Supplementary Table 10](#)), initially defining overlap between an eQTL and
148 pQTL as high linkage disequilibrium (LD) ($r^2 \geq 0.8$) between the lead pQTL and eQTL variants.
149 40% ($n = 224$) of *cis* pQTLs were eQTLs for the same gene in ≥ 1 tissue or cell-type
150 ([Supplementary Table 8](#)). The greatest overlaps were in whole blood ($n = 117$), liver ($n = 70$) and
151 lymphoblastoid cell-lines (LCLs) ($n = 52$), consistent with biological expectation, but also likely
152 driven by the larger eQTL study sample sizes for these cell-types. To examine whether the
153 same causal variant was likely to underlie overlapping eQTLs and pQTLs, we performed
154 colocalisation testing ([Methods](#)). Of 228 non-*HLA* pQTLs for which testing was possible,
155 colocalisation in ≥ 1 tissue or cell-type was highly likely (posterior probability[PP] > 0.8) in 179
156 (78.5%) and the most likely explanation (PP > 0.5) in 197 (86.4%) ([Supplementary Table 8](#)).
157 *Cis* pQTLs were significantly enriched for eQTLs for the corresponding gene ($p < 0.0001$)
158 ([Methods](#), [Supplementary Table 11](#)). To address the converse (i.e., to what extent do eQTLs
159 translate into pQTLs), we used a set of well-powered eQTL studies in relevant tissues (whole
160 blood, LCLs, liver and monocytes¹⁶⁻¹⁹). Of the strongest *cis* eQTLs ($p < 1.5 \times 10^{-11}$), 12.2% of

161 those in whole blood were also *cis* pQTLs, 21.3% for LCLs, 14.8% for liver and 14.7% for
162 monocytes.

163

164 Comparisons between eQTL and pQTL studies have inherent limitations, including differences
165 in the tissues, sample sizes and technological platforms used. Moreover, plasma protein levels
166 may not reflect levels within tissues or cells. Nevertheless, our data suggest that genetic effects
167 on plasma protein abundance are often, but not exclusively, driven by regulation of mRNA.
168 *Cis* pQTLs without corresponding *cis* eQTLs may reflect genetic effects on processes other
169 than transcription, including protein degradation, binding, secretion, or clearance from
170 circulation.

171

172 **Using *trans* pQTLs to illuminate biological pathways and disease** 173 **pathobiology**

174 *Trans* pQTLs are useful for understanding biological relationships between proteins,
175 particularly when the causal gene at the *trans*-associated locus can be identified. Of the 764
176 protein-associated regions, 262 had *trans* associations with 1,104 proteins (Supplementary
177 Table 4, 12). There was no enrichment of cross-reactivity in SOMAmers with a *trans* pQTL
178 versus those without (Supplementary Note). We replicated previously reported *trans*
179 associations including *TMPRSS6* with transferrin receptor protein 1²⁰ and *SORT1* with
180 granulins²¹ and identified several novel biologically plausible *trans* associations
181 (Supplementary Table 13), including known or presumed ligand:receptor pairs (e.g., the
182 *CD320* gene region, which encodes the transcobalamin receptor, was associated with
183 transcobalamin-2 levels).

184

185 Most (82%) *trans* loci were associated with <4 proteins, but 12 ‘hotspot’ regions were
186 associated with >20 (Figure 1a, Extended Data Figure 3b), including well-known pleiotropic
187 loci (e.g., *ABO*, *CFH*, *APOE*, *KLKB1*) and loci associated with many correlated proteins (e.g.,
188 the *ZFPM2* locus encoding the transcription factor FOG2). Similar pleiotropy at these loci has
189 been seen in other plasma pQTL studies²²⁻²⁴, albeit with fewer proteins due to more limited
190 assay breadth. rs28929474:T in *SERPINA1* was associated with 13 proteins at $p < 1.5 \times 10^{-11}$ and
191 a further six at $p < 5 \times 10^{-8}$ (Figure 2). This missense variant (the ‘Z-allele’, p.Glu366Lys) results
192 in defective secretion and intracellular accumulation of alpha1-antitrypsin (A1AT), an anti-
193 protease. ZZ homozygotes have deficiency of circulating A1AT and increased risk of
194 emphysema, liver cirrhosis and vasculitis. The ‘protease-antiprotease’ hypothesis posits that
195 these clinical manifestations result from unchecked protease activity. However, our discovery
196 of multiple *trans*-associated proteins at this locus highlights additional pathways potentially
197 relevant to pathogenesis, a hypothesis supported by accumulating data²⁵.

198

199 GWAS have identified thousands of loci associated with common diseases, but the
200 mechanisms by which most variants influence disease susceptibility await discovery. To
201 identify intermediate links between genotype and disease, we overlapped pQTLs with disease-
202 associated genetic variants identified through GWAS. 88 of our sentinel pQTL variants were
203 in high LD ($r^2 \geq 0.8$) with sentinel disease-associated variants (Supplementary Table 14),
204 including 30 with *cis* associations, 54 with *trans* associations and 4 with both. Since some
205 genetic loci are associated with multiple diseases, these 88 genetic loci represent 253 distinct
206 genotype-disease associations. Overlap of a pQTL and a disease association signal does not
207 necessarily imply that the same genetic variant underlies both traits, since there may be distinct
208 causal variants for each trait that are in LD with one another. We therefore performed
209 colocalisation testing (Methods). Of 108 locus-disease associations for which testing was

210 possible (excluding the MHC region), colocalisation was highly likely (PP>0.8) for 96
211 (88.9%), and the most likely explanation (PP>0.5) for 106 (98.1%) (Supplementary Table 14).

212

213 *Trans* pQTLs that overlap with disease associations can highlight previously unsuspected
214 candidate proteins through which genetic loci may influence disease risk. To help identify such
215 candidates, we applied the ProGeM framework²⁶ (Methods, Supplementary Table 12,
216 Extended Data Figure 5). We show that an inflammatory bowel disease (IBD) risk allele²⁷⁻²⁸
217 (rs3197999:A, missense p.Arg703Cys) in *MST1* on chromosome 3, that decreases plasma
218 MST1 levels²⁹, is a *trans* pQTL for eight additional proteins (Supplementary Table 4, Figure
219 3). Notably, genes that encode three of these proteins (*PRDMI*, *FASLG*, and *DOCK9*) each lie
220 within 500kb of IBD GWAS loci where the causal gene is ambiguous³⁰. For instance, the IBD-
221 associated variant rs6911490 lies on chromosome 6 in the intergenic region between *PRDMI*
222 (encoding BLIMP1, a master regulator of immune cell differentiation) and *ATG5* (involved in
223 autophagy) (Figure 3c). Neither fine-mapping nor eQTL colocalisation analyses have
224 unequivocally resolved the causal gene at this locus³⁰; both *PRDMI* and *ATG5* are plausible
225 candidates. Our data provide support for *PRDMI*.

226

227 Anti-neutrophil cytoplasmic antibody-associated vasculitis (AAV) is an autoimmune disease
228 characterised by vascular inflammation and autoantibodies to the neutrophil proteases
229 proteinase-3 (PR3) or myeloperoxidase. GWAS reveal distinct genetic signals according to
230 antibody specificity³¹, with variants near *PRTN3* (encoding PR3) and at the Z-allele of
231 *SERPINA1* (encoding alpha1-antitrypsin, an inhibitor of PR3) associated specifically with
232 PR3-antibody positive AAV. The SOMAscan assay has two SOMAmers targeting PR3; we
233 identified a *cis* pQTL signal immediately upstream of *PRTN3* for both (Supplementary Table
234 4, Figures 4a-b). Conditional analysis revealed multiple independently associated variants

235 (Supplementary Table 5), one of which (rs7254911) was in high LD with the PR3+ vasculitis
236 tag SNPs (Supplementary Note). We show that the vasculitis risk allele at *PRTN3* is associated
237 with higher plasma levels of PR3 (Supplementary Note Table 4).

238

239 For one PR3 SOMAmer, we also found a *trans* pQTL at *SERPINA1*, with the Z-allele
240 associating with lower plasma PR3 (Figure 4a). To understand the SOMAmer-specific nature
241 of this signal, we assayed the relative affinity of these SOMAmers for the free and complexed
242 states of PR3 and A1AT (which binds and inhibits proteases including PR3). We found that
243 the SOMAmer showing *cis* and *trans* associations predominantly measures the PR3:A1AT
244 complex rather than free PR3, whereas the SOMAmer with only *cis* association measures both
245 the free and complexed forms. Importantly, neither SOMAmer bound free A1AT,
246 demonstrating that the *SERPINA1* pQTL did not reflect non-specific cross-reactivity
247 (Supplementary Note).

248

249 These data show that the vasculitis risk allele at *PRTN3* increases total PR3 plasma levels,
250 consistent with its effect on *PRTN3* mRNA abundance in whole blood in GTEx data³². The
251 *SERPINA1* Z-allele results in a reduced proportion of PR3 bound to A1AT. We thus
252 demonstrate how altered availability of PR3, conferred by two independent genetic
253 mechanisms, is a key susceptibility factor for breaking immune tolerance to PR3 and the
254 development of PR3+ vasculitis (Figure 4c).

255

256 **Causal evaluation of candidate proteins in disease**

257 Association of plasma protein levels with disease risk does not necessarily imply causation. To
258 help establish causality, we employed the principle of Mendelian randomisation (MR)¹⁰
259 (Extended Data Figure 6). In contrast with observational studies, which are liable to

260 confounding and/or reverse causation, MR analysis can be akin to a ‘natural’ randomised
261 controlled trial, exploiting the random allocation of alleles at conception. Consequently, if a
262 genetic variant that specifically influences levels of a protein is also associated with disease
263 risk, then it provides strong evidence of the protein’s causal role. For example, serum levels of
264 PSP-94 (MSMB) are lower in patients with prostate cancer³³, but it is debated whether this
265 association is correlative or causal. We identified a *cis* pQTL associated with lower PSP-94
266 plasma levels that overlaps with the prostate cancer susceptibility variant rs10993994³⁴,
267 supporting a protective role for PSP-94 in prostate cancer (Supplementary Table 14).

268

269 Next, we leveraged multi-variant MR analysis methods to distinguish causal genes among
270 multiple plausible candidates at disease loci, exemplified by the *IL1RL1-IL18R1* locus, which
271 has been associated with a range of immune-mediated diseases including atopic dermatitis³⁵.
272 We identified four proteins that each had *cis* pQTLs at this locus (Supplementary Table 4), and
273 created a genetic score for each protein (Methods). Initial ‘one-protein-at-a-time’ analysis
274 identified associations of the scores for IL18R1 ($p=9.3 \times 10^{-72}$) and IL1RL1 ($p=5.7 \times 10^{-27}$) with
275 atopic dermatitis risk (Figure 5a), and a weak association for IL1RL2 ($p=0.013$). We then
276 mutually adjusted these associations for one another to account for the effects of the variants
277 on multiple proteins. While the association of IL18R1 remained significant ($p=1.5 \times 10^{-28}$), the
278 association of IL1RL1 ($p=0.01$) was attenuated. In contrast, the association of IL1RL2
279 ($p=1.1 \times 10^{-69}$) became much stronger, suggesting that IL1RL2 and IL18R1 underlie atopic
280 dermatitis risk at this locus.

281

282 MMP-12 plays a key role in lung tissue damage, and MMP-12 inhibitors are being tested for
283 chronic obstructive pulmonary disease³⁶⁻³⁷. We created a multi-allelic genetic score that
284 explains 14% of the variation in plasma macrophage metalloelastase (MMP-12) levels

285 (Methods). Observational studies reveal an association of higher levels of plasma MMP-12
286 with recurrent cardiovascular events³⁸⁻³⁹, stimulating interest in development of MMP-12
287 inhibitors for cardiovascular disease. In contrast, we found that genetic predisposition to higher
288 MMP-12 levels is associated with *decreased* coronary disease risk ($p=2.8 \times 10^{-13}$) (Figure 5b)
289 and *decreased* large artery atherosclerotic stroke risk⁴⁰. Understanding the discordance
290 between the observational epidemiology and the genetic risk score will be important given the
291 therapeutic interest in this target.

292

293 **Drug target prioritisation**

294 Drugs directed at therapeutic targets implicated by human genetic data have a greater
295 likelihood of success⁴¹. Of the proteins for which we identified a pQTL, 244 (17%) are
296 established drug targets in the Informa Pharmaprojects database (Citeline) (Supplementary
297 Table 15). 31 pQTLs for drug target proteins were highly likely to colocalise (posterior
298 probability > 0.8) with a disease GWAS locus, including some that are targets of approved drugs
299 such as tocilizumab (anti-IL6R) and ustekinumab (anti-IL12/23) (Supplementary Table 16a).

300

301 To identify additional indications for existing drugs, we investigated disease associations of
302 pQTLs for proteins already targeted by licensed drugs. Our results suggest potential drug ‘re-
303 purposing’ opportunities. For example, we identified a *cis* pQTL for RANK (encoded by
304 *TNFRSF11A*) at a variant (rs884205) associated with Paget’s disease, a condition characterised
305 by excessive bone turnover, deformity and fracture (Supplementary Table 16b). Standard
306 Paget’s disease treatment consists of osteoclast inhibition with bisphosphonates, originally
307 developed as anti-osteoporotic drugs. Denosumab, another anti-osteoporosis drug, is a
308 monoclonal antibody targeting RANKL, the ligand for RANK. Our data suggest denosumab

309 may be an alternative for Paget's disease patients in whom bisphosphonates are contra-
310 indicated, a hypothesis supported by clinical case reports⁴³⁻⁴⁴.

311

312 Next we evaluated targets for drugs currently under development, such as GP1BA, the receptor
313 for von Willebrand factor. Drugs targeting GP1BA are in pre-clinical development as anti-
314 thrombotic agents and in phase 2 trials for thrombotic thrombocytopenic purpura. We
315 identified a *trans* pQTL for GP1BA at the pleiotropic *SH2B3/BRAP* locus, which is associated
316 with platelet count⁴⁵, myocardial infarction (MI) and stroke (Supplementary Table 16b; r^2 from
317 sentinel pQTL variant to lead platelet count, MI, and stroke variants is 0.91, 1.0, and 1.0,
318 respectively). The risk allele for cardiovascular disease increases both plasma GP1BA and
319 platelet count, suggesting a mechanism by which this locus affects disease susceptibility. As a
320 confirmation of the link between GP1BA and platelet count, we found a directionally
321 concordant *cis* pQTL for GP1BA at a platelet count-associated variant (Supplementary Table
322 16). Collectively, these results suggest that targeting GP1BA may be efficacious in conditions
323 characterised by platelet aggregation such as arterial thrombosis. More generally, our data
324 provide a substrate for generating hypotheses about potential therapeutic targets through
325 linking genetic factors to disease via specific proteins.

326

327 **DISCUSSION**

328 This study elucidates the genetic control of the human plasma proteome and uncovers
329 intermediate molecular pathways that connect the genome to disease endpoints. We applied
330 our discoveries to evaluate causal roles for proteins in important diseases using the principle
331 of Mendelian randomisation (MR). Proteins provide an ideal paradigm for MR analysis
332 because they are under proximal genetic control. However, application of protein-based MR
333 has been constrained by limited availability of suitable genetic instruments, a bottleneck

334 remedied by our data. Overall, our study foreshadows major advances in post-genomic science
335 through increasing application of novel bioassay technologies to population biobanks.

336 REFERENCES

- 337 1. Albert, F. W. & Kruglyak, L. The role of regulatory variation in complex traits and
338 disease. *Nat. Rev. Genet.* **16**, 197–212 (2015).
- 339 2. Liu, Y. *et al.* Quantitative variability of 342 plasma proteins in a human twin
340 population. *Mol. Syst. Biol.* **11**, 786 (2015).
- 341 3. Melzer, D. *et al.* A genome-wide association study identifies protein quantitative trait
342 loci (pQTLs). *PLoS Genet* **4**, e1000072 (2008).
- 343 4. Enroth, S., Johansson, Å., Enroth, S. B. & Gyllensten, U. Strong effects of genetic and
344 lifestyle factors on biomarker variation and use of personalized cutoffs. *Nat Commun* **5**, 4684
345 (2014).
- 346 5. Deming, Y. *et al.* Genetic studies of plasma analytes identify novel potential
347 biomarkers for several complex traits. *Sci. Rep.* **6**, 18092 (2016).
- 348 6. Hause, R. J. *et al.* Identification and validation of genetic variants that influence
349 transcription factor and cell signaling protein levels. *Am J Hum Genet* **95**, 194–208 (2014).
- 350 7. Wu, L. *et al.* Variation and genetic control of protein abundance in humans. *Nature*
351 **499**, 79–82 (2013).
- 352 8. Battle, A. *et al.* Impact of regulatory variation from RNA to protein. *Science.* **347**, 644–
353 7 (2015).
- 354 9. Rohloff, J. C. *et al.* Nucleic acid ligands with protein-like side chains: modified
355 aptamers and their use as diagnostic and therapeutic agents. *Mol. Ther. Nucleic Acids* **3**, e201
356 (2014).
- 357 10. Burgess, S. *et al.* Using published data in Mendelian randomization: a blueprint for
358 efficient identification of causal risk factors. *Eur. J. Epidemiol.* **30**, 543–52 (2015).
- 359 11. Stranger, B. E. *et al.* Patterns of cis regulatory variation in diverse human populations.
360 *PLoS Genet.* **8**, e1002639 (2012).
- 361 12. Montgomery, S. B. & Dermitzakis, E. T. From expression QTLs to personalized
362 transcriptomics. *Nat. Rev. Genet.* **12**, 277–282 (2011).
- 363 13. Lundberg, M., Eriksson, A., Tran, B., Assarsson, E. & Fredriksson, S. Homogeneous
364 antibody-based proximity extension assays provide sensitive and specific detection of low-
365 abundant proteins in human blood. *Nucleic Acids Res.* **39**, e102 (2011).
- 366 14. Walter, K. *et al.* The UK10K project identifies rare variants in health and disease.
367 *Nature* **526**, 82–90 (2015).
- 368 15. Astle, W. J. *et al.* The allelic landscape of human blood cell trait variation and links to
369 common complex disease. *Cell* **167**, 1415–1429.e19 (2016).

- 370 16. Westra, H.-J. *et al.* Systematic identification of trans eQTLs as putative drivers of
371 known disease associations. *Nat Genet* **45**, 1238–1243 (2013).
- 372 17. Lappalainen, T. *et al.* Transcriptome and genome sequencing uncovers functional
373 variation in humans. *Nature* **501**, 506–511 (2013).
- 374 18. Schadt, E. E. *et al.* Mapping the genetic architecture of gene expression in human liver.
375 *PLoS Biol.* **6**, e107 (2008).
- 376 19. Zeller, T. *et al.* Genetics and beyond – the transcriptome of human monocytes and
377 disease susceptibility. *PLoS One* **5**, e10693 (2010).
- 378 20. Nai, A. *et al.* TMPRSS6 rs855791 modulates hepcidin transcription in vitro and serum
379 hepcidin levels in normal individuals. *Blood* **118**, 4459–62 (2011).
- 380 21. Carrasquillo, M. M. *et al.* Genome-wide screen identifies rs646776 near sortilin as a
381 regulator of progranulin levels in human plasma. *Am. J. Hum. Genet.* **87**, 890–897 (2010).
- 382 22. Suhre, K. *et al.* Connecting genetic risk to disease end points through the human blood
383 plasma proteome. *Nat. Commun.* **8**, 14357 (2017).
- 384 23. Yao, C. *et al.* Genome-wide association study of plasma proteins identifies putatively
385 causal genes, proteins, and pathways for cardiovascular disease. *bioRxiv* (2017).
386 doi:10.1101/136523
- 387 24. de Vries, P. S. *et al.* Whole-genome sequencing study of serum peptide levels: the
388 Atherosclerosis Risk in Communities study. *Hum. Mol. Genet.* **26**, 3442–3450 (2017).
- 389 25. Gooptu, B., Dickens, J. A. & Lomas, D. A. The molecular and cellular pathology of α_1 -
390 antitrypsin deficiency. *Trends Mol. Med.* **20**, 116–27 (2014).
- 391 26. Stacey, D. *et al.* ProGeM: A framework for the prioritisation of candidate causal genes
392 at molecular quantitative trait loci. *bioRxiv* 230094 (2017). doi:10.1101/230094
- 393 27. Jostins, L. *et al.* Host–microbe interactions have shaped the genetic architecture of
394 inflammatory bowel disease. *Nature* **491**, 119–124 (2012).
- 395 28. Liu, J. Z. *et al.* Association analyses identify 38 susceptibility loci for inflammatory
396 bowel disease and highlight shared genetic risk across populations. *Nat. Genet.* **47**, 979–986
397 (2015).
- 398 29. Di Narzo, A. F. *et al.* High-throughput characterization of blood serum proteomics of
399 IBD patients with respect to aging and genetic factors. *PLoS Genet.* **13**, e1006565 (2017).
- 400 30. Huang, H. *et al.* Fine-mapping inflammatory bowel disease loci to single-variant
401 resolution. *Nature* **547**, 173–178 (2017).
- 402 31. Lyons, P. A. *et al.* Genetically distinct subsets within ANCA-associated vasculitis. *N.*
403 *Engl. J. Med.* **367**, 214–223 (2012).
- 404 32. Aguet, F. *et al.* Genetic effects on gene expression across human tissues. *Nature* **550**,
405 204–213 (2017).

- 406 33. Grönberg, H. *et al.* Prostate cancer screening in men aged 50–69 years (STHLM3): a
407 prospective population-based diagnostic study. *Lancet Oncol.* **16**, 1667–1676 (2015).
- 408 34. Eeles, R. A. *et al.* Multiple newly identified loci associated with prostate cancer
409 susceptibility. *Nat. Genet.* **40**, 316–321 (2008).
- 410 35. Paternoster, L. *et al.* Multi-ancestry genome-wide association study of 21,000 cases
411 and 95,000 controls identifies new risk loci for atopic dermatitis. *Nat. Genet.* **47**, 1449–56
412 (2015).
- 413 36. Dahl, R. *et al.* Effects of an oral MMP-9 and -12 inhibitor, AZD1236, on biomarkers
414 in moderate/severe COPD: A randomised controlled trial. *Pulm. Pharmacol. Ther.* **25**, 169–
415 177 (2012).
- 416 37. Churg, A. *et al.* Effect of an MMP-9/MMP-12 inhibitor on smoke-induced emphysema
417 and airway remodelling in guinea pigs. *Thorax* **62**, 706–713 (2007).
- 418 38. Ganz, P. *et al.* Development and validation of a protein-based risk score for
419 cardiovascular outcomes among patients with stable coronary heart disease. *JAMA* **315**, 2532–
420 41 (2016).
- 421 39. Goncalves, I. *et al.* Elevated plasma levels of MMP-12 are associated with
422 atherosclerotic burden and symptomatic cardiovascular disease in subjects with type 2 diabetes.
423 *Arterioscler. Thromb. Vasc. Biol.* **35**, 1723–1731 (2015).
- 424 40. Traylor, M. *et al.* A novel MMP12 locus is associated with large artery atherosclerotic
425 stroke using a genome-wide age-at-onset informed approach. *PLoS Genet.* **10**, e1004469
426 (2014).
- 427 41. Nelson, M. R. *et al.* The support of human genetic evidence for approved drug
428 indications. *Nat. Genet.* **47**, 856–860 (2015).
- 429 42. Albagha, O. M. E. *et al.* Genome-wide association study identifies variants at CSF1,
430 OPTN and TNFRSF11A as genetic risk factors for Paget’s disease of bone. *Nat. Genet.* **42**,
431 520–524 (2010).
- 432 43. Schwarz, P., Rasmussen, A. Q., Kvist, T. M., Andersen, U. B. & Jørgensen, N. R.
433 Paget’s disease of the bone after treatment with Denosumab: a case report. *Bone* **50**, 1023–5
434 (2012).
- 435 44. Polyzos, S. A. *et al.* Denosumab treatment for juvenile Paget’s disease: results from
436 two adult patients with osteoprotegerin deficiency (‘Balkan’ mutation in the TNFRSF11B
437 gene). *J. Clin. Endocrinol. Metab.* **99**, 703–707 (2014).
- 438 45. Gieger, C. *et al.* New gene functions in megakaryopoiesis and platelet formation.
439 *Nature* **480**, 201–208 (2011).
- 440
- 441

442 **ONLINE METHODS**

443 **Study participants**

444 The INTERVAL study comprised about 50,000 participants nested within a randomised trial
445 of varying blood donation intervals⁴⁶. Between mid-2012 and mid-2014, whole-blood donors
446 aged 18 years and older were consented and recruited at 25 centers of England's National
447 Health Service Blood and Transplant (NHSBT). Participants completed an online
448 questionnaire including questions about demographic characteristics (e.g., age, sex, ethnic
449 group), anthropometry (height, weight), lifestyle (e.g., alcohol and tobacco consumption) and
450 diet. Participants were generally in good health because blood donation criteria exclude people
451 with a history of major diseases (such as myocardial infarction, stroke, cancer, HIV, and
452 hepatitis B or C) and those who have had recent illness or infection. For protein assays, we
453 randomly selected two non-overlapping subcohorts of 2,731 and 831 participants from
454 INTERVAL. After genetic QC, 3,301 participants (2,481 and 820 in the two subcohorts)
455 remained for analysis ([Supplementary Table 17](#)).

456

457 **Plasma sample preparation**

458 Sample collection procedures for INTERVAL have been described previously⁴⁷. In brief, blood
459 samples for research purposes were collected in 6ml EDTA tubes using standard venepuncture
460 protocols. The tubes were inverted three times and transferred at room temperature to UK
461 Biocentre (Stockport, UK) for processing. Plasma was extracted into two 0.8ml plasma aliquots
462 by centrifugation and subsequently stored at -80°C prior to use.

463

464 **Protein measurements**

465 We used a multiplexed, aptamer-based approach (SOMAscan assay) to measure the relative
466 concentrations of 3,622 plasma proteins/protein complexes assayed using 4,034 modified
467 aptamers (“SOMAmer reagents”, hereafter referred to as ‘SOMAmers’; Supplementary Table
468 18). The assay extends the lower limit of detectable protein abundance afforded by
469 conventional approaches (e.g., immunoassays), measuring both extracellular and intracellular
470 proteins (including soluble domains of membrane-associated proteins), with a bias towards
471 proteins likely to be found in the human secretome (Extended Data Figure 7a)^{9,48}. The proteins
472 cover a wide range of molecular functions (Extended Data Figure 7b). The selection of proteins
473 on the platform reflects both the availability of purified protein targets and a focus on proteins
474 suspected to be involved in pathophysiology of human disease.

475

476 Aliquots of 150 µl of plasma were sent on dry ice to SomaLogic Inc. (Boulder, Colorado, US)
477 for protein measurement. Assay details have been previously described⁴⁸⁻⁵⁰ and a technical
478 white paper with further information can be found at the manufacturer’s website
479 ([http://somalogic.com/wp-content/uploads/2017/06/SSM-002-Technical-White-](http://somalogic.com/wp-content/uploads/2017/06/SSM-002-Technical-White-Paper_010916_LSM1.pdf)
480 [Paper_010916_LSM1.pdf](http://somalogic.com/wp-content/uploads/2017/06/SSM-002-Technical-White-Paper_010916_LSM1.pdf)). In brief, modified single-stranded DNA SOMAmers are used to
481 bind to specific protein targets that are then quantified using a DNA microarray. Protein
482 concentrations are quantified as relative fluorescent units.

483

484 Quality control (QC) was performed at the sample and SOMAmer level using control aptamers,
485 as well as calibrator samples. At the sample level, hybridisation controls on the microarray
486 were used to correct for systematic variability in hybridisation, while the median signal over
487 all features assigned to one of three dilution sets (40%, 1% and 0.005%) was used to correct
488 for within-run technical variability. The resulting hybridisation scale factors and median scale
489 factors were used to normalise data across samples within a run. The acceptance criteria for

490 these values are between 0.4 and 2.5 based on historical runs. SOMAmer-level QC made use
491 of replicate calibrator samples using the same study matrix (plasma) to correct for between-run
492 variability. The acceptance criterion for each SOMAmer was that the calibration scale factor
493 be less than 0.4 from the median for each of the plates run. In addition, at the plate level, the
494 acceptance criteria were that the median of the calibration scale factors be between 0.8 and 1.2,
495 and that 95% of individual SOMAmers be less than 0.4 from the median within the plate.

496

497 In addition to QC processes routinely conducted by SomaLogic, we measured protein levels of
498 30 and 10 pooled plasma samples randomly distributed across plates for subcohort 1 and
499 subcohort 2, respectively. Laboratory technicians were blinded to the presence of pooled
500 samples. This approach enabled estimation of the reproducibility of the protein assays. We
501 calculated CVs for each SOMAmer within each subcohort by dividing the standard deviation
502 by the mean of the pooled plasma sample protein read-outs. In addition to passing SomaLogic
503 QC processes, we required SOMAmers to have a $CV \leq 20\%$ in both subcohorts. Eight non-
504 human protein targets were also excluded, leaving 3,283 SOMAmers (mapping to 2,994 unique
505 proteins/protein complexes) for inclusion in the GWAS.

506

507 Protein mapping to UniProt identifiers and gene names was provided by SomaLogic. Mapping
508 to Ensembl gene IDs and genomic positions was performed using Ensembl Variant Effect
509 Predictor v83 (VEP)⁵¹. Protein subcellular locations were determined by exporting the
510 subcellular location annotations from UniProt⁵². If the term ‘membrane’ was included in the
511 descriptor, the protein was considered to be a membrane protein, whereas if the term ‘secreted’
512 (but not ‘membrane’) was included in the descriptor, the protein was considered to be a secreted
513 protein. Proteins not annotated as either membrane or secreted proteins were classified (by

514 inference) as intracellular proteins. Proteins were mapped to molecular functions using gene
515 ontology annotations⁵³ from UniProt.

516

517 **Non-genetic associations of proteins**

518 To provide confidence in the reproducibility of the protein assays, we attempted to replicate
519 the associations with age or sex of 45 proteins previously reported by Ngo *et al* and 40 reported
520 by Menni *et al*^{49,54}. We used Bonferroni-corrected p -value thresholds of $p=1.1 \times 10^{-3}$ (0.05/45)
521 and $p=1.2 \times 10^{-3}$ (0.05/40) respectively. Relative protein abundances were rank-inverse
522 normalised within each subcohort and linear regression was performed using age, sex, BMI,
523 natural log of estimated glomerular filtration rate (eGFR) and subcohort as independent
524 variables.

525

526 **Genotyping and imputation**

527 The genotyping protocol and QC for the INTERVAL samples (n~50,000) have been described
528 previously in detail¹⁵. Briefly, DNA extracted from buffy coat was used to assay approximately
529 830,000 variants on the Affymetrix Axiom UK Biobank genotyping array at Affymetrix (Santa
530 Clara, California, US). Genotyping was performed in multiple batches of approximately 4,800
531 samples each. Sample QC was performed including exclusions for sex mismatches, low call
532 rates, duplicate samples, extreme heterozygosity and non-European descent. An additional
533 exclusion made for this study was of one participant from each pair of close (first- or second-
534 degree) relatives, defined as $\hat{\pi} > 0.187$. Identity-by-descent was estimated using a subset of
535 variants with a call rate >99% and MAF >5% in the merged dataset of both subcohorts, pruned
536 for linkage disequilibrium (LD) using PLINK v1.9⁵⁵. Numbers of participants excluded at each
537 stage of the genetic QC are summarised in [Extended Data Figure 1](#). Multi-dimensional scaling
538 was performed using PLINK v1.9 to create components to account for ancestry in genetic

539 analyses.

540

541 Prior to imputation, additional variant filtering steps were performed to establish a high-quality
542 imputation scaffold. In summary, 654,966 high quality variants (autosomal, non-
543 monomorphic, bi-allelic variants with Hardy Weinberg Equilibrium (HWE) $p > 5 \times 10^{-6}$, with a
544 call rate of $>99\%$ across the INTERVAL genotyping batches in which a variant passed QC,
545 and a global call rate of $>75\%$ across all INTERVAL genotyping batches) were used for
546 imputation. Variants were phased using SHAPEIT3 and imputed using a combined 1000
547 Genomes Phase 3-UK10K reference panel. Imputation was performed via the Sanger
548 Imputation Server (<https://imputation.sanger.ac.uk>) resulting in 87,696,888 imputed variants.

549

550 Prior to genetic association testing, variants were filtered in each subcohort separately using
551 the following exclusion criteria: (1) imputation quality (INFO) score < 0.7 , (2) minor allele
552 count < 8 , (3) HWE $p < 5 \times 10^{-6}$. In the small number of cases where imputed variants had the
553 same genomic position (GRCh37) and alleles, the variant with the lowest INFO score was
554 removed. 10,572,788 variants passing all filters in both subcohorts were taken forward for
555 analysis (Extended Data Figure 1).

556

557 **Genome-wide association study**

558 Within each subcohort, relative protein abundances were first natural log-transformed. Log-
559 transformed protein levels were then adjusted in a linear regression for age, sex, duration
560 between blood draw and processing (binary, ≤ 1 day/ >1 day) and the first three principal
561 components of ancestry from multi-dimensional scaling. The protein residuals from this linear
562 regression were then rank-inverse normalised and used as phenotypes for association testing.
563 Simple linear regression using an additive genetic model was used to test genetic associations.

564 Association tests were carried out on allelic dosages to account for imputation uncertainty (“-
565 method expected” option) using SNPTEST v2.5.2⁵⁶.

566

567 **Meta-analysis and statistical significance**

568 Association results from the two subcohorts were combined via fixed-effects inverse-variance
569 meta-analysis combining the betas and standard errors using METAL⁵⁷. Genetic associations
570 were considered to be genome-wide significant based on a conservative strategy requiring
571 associations to have (i) a meta-analysis p -value $< 1.5 \times 10^{-11}$ (genome-wide threshold of $p = 5 \times 10^{-8}$
572 ⁸ Bonferroni-corrected for 3,283 aptamers tested), (ii) at least nominal significance ($p < 0.05$)
573 in both subcohorts, and (iii) consistent direction of effect across subcohorts. We did not observe
574 significant genomic inflation (mean inflation factor was 1.0, standard deviation=0.01)
575 (Extended Data Figure 2d).

576

577 **Refinement of significant regions**

578 To identify distinct non-overlapping regions associated with a given SOMAmer, we first
579 defined a 1Mb region around each significant variant for that SOMAmer. Starting with the
580 region containing the variant with the smallest p -value, any overlapping regions were then
581 merged and this process was repeated until no more overlapping 1Mb regions remained. The
582 variant with the lowest p -value for each region was assigned as the “regional sentinel variant”.
583 Due to the complexity of the Major Histocompatibility Region (MHC) region, we treated the
584 extended MHC region (chr6:25.5-34.0Mb) as one region. To identify whether a region was
585 associated with multiple SOMAmers, we used an LD-based clumping approach. Regional
586 sentinel variants in high LD ($r^2 \geq 0.8$) with each other were combined together into a single
587 region.

588

589 **Conditional analyses**

590 To identify conditionally significant signals, we performed approximate genome-wide step-
591 wise conditional analysis using GCTA v1.25.2⁵⁸ using the “cojo-slc” option. We used the same
592 conservative significance threshold of $p=1.5 \times 10^{-11}$ as for the univariable analysis. As inputs for
593 GCTA, we used the summary statistics (i.e. betas and standard errors) from the meta-analysis.
594 Correlation between variants was estimated using the ‘hard-called’ genotypes (where a
595 genotype was called if it had a posterior probability of >0.9 following imputation or set to
596 missing otherwise) in the merged genetic dataset, and only variants also passing the univariable
597 genome-wide threshold ($p < 1.5 \times 10^{-11}$) were considered for step-wise selection. As the
598 conditional analyses use different data inputs to the univariable analysis (i.e. summarised rather
599 than individual-level data), there were some instances where the conditional analysis failed to
600 include in the step-wise selection sentinel variants that were only just statistically significant
601 in the univariable analysis. In these instances ($n=28$), we re-conducted the joint model
602 estimation without step-wise selection in GCTA, using the variants identified by the
603 conditional analysis in addition to the regional sentinel variant. We report and highlight these
604 cases in Supplementary Table 5.

605

606 **Replication of previous pQTLs**

607 We attempted to identify all previously reported pQTLs from GWAS and to assess whether
608 they replicated in our study. We used the NCBI Entrez programming utility in R (rentrez) to
609 perform a literature search for pQTL studies published from 2008 onwards. We searched for
610 the following terms: ‘pQTL’, ‘pQTLs’, and ‘protein quantitative trait locus’. We supplemented
611 this search by filtering out GWAS associations from the NHGRI-EBI GWAS Catalog v.1.0.1⁵⁹
612 (<https://www.ebi.ac.uk/gwas/>, downloaded November 2017), which has all phenotypes
613 mapped to the Experimental Factor Ontology (EFO)⁶⁰, by restricting to those with EFO

614 annotations relevant to protein biomarkers (e.g., ‘protein measurement’, EFO_0004747).
615 Studies identified through both approaches were manually filtered to include only studies that
616 profiled plasma or serum samples and to exclude studies not assessing proteins. We recorded
617 basic summary information for each study including the assay used, sample size and number
618 of proteins with pQTLs (Supplementary Table 19). To reduce the impact of ethnic differences
619 in allele frequencies on replication rate estimates, we filtered studies to include only
620 associations reported in European-ancestry populations. We then manually extracted summary
621 data on all reported associations from the manuscript or the supplementary material. This
622 included rsID, protein UniProt ID, *p*-values, and whether the association is *cis/trans*
623 (Supplementary Table 20).

624

625 To assess replication we first identified the set of unique UniProt IDs that were also assayed
626 on the SOMAscan panel. For previous studies that used SomaLogic technology, we refined
627 this match to the specific aptamer used. We then clumped associations into distinct loci using
628 the same method that we applied to our pQTLs (see **Refinement of significant regions**). For
629 each locus, we asked if the sentinel SNP or a proxy ($r^2 > 0.6$) was associated with the same
630 protein/aptamer in our study at a defined significance threshold. For our primary assessment,
631 we used a *p*-value threshold of 10^{-4} (Supplementary Table 21). We also performed sensitivity
632 analyses to explore factors that influence replication rate (Supplementary Note).

633

634 **Replication study using Olink assay**

635 To test replication of 163 pQTLs for 116 proteins, we performed protein measurements using
636 an alternative assay, i.e., a proximity extension assay method (Olink Bioscience, Uppsala,
637 Sweden)⁴ in an additional subcohort of 4,998 INTERVAL participants. Proteins were
638 measured using three 92-protein ‘panels’ – ‘inflammatory’, ‘cvd2’ and ‘cvd3’ (10 proteins

639 were assayed on more than 1 panel). 4,902, 4,947 and 4,987 samples passed quality control for
640 the ‘inflammatory’, ‘cvd2’ and ‘cvd3’ panels, respectively, of which, 712, 715 and 721 samples
641 were from individuals included in our primary pQTL analysis using the SOMAscan assay.
642 Normalised protein levels (‘NPX’) were regressed on age, sex, plate, time from blood draw to
643 processing (in days), and season (categorical – ‘Spring’, ‘Summer’, ‘Autumn’, ‘Winter’). The
644 residuals were then rank-inverse normalized. Genotype data was processed as described earlier.
645 Linear regression of the rank-inversed normalised residuals on genotype was carried out in
646 SNPTEST with the first three components of multi-dimensional scaling as covariates to adjust
647 for ancestry. pQTLs were considered to have replicated if they met a p -value threshold
648 Bonferroni-corrected for the number of tests ($p < 3.1 \times 10^{-4}$; $0.05/163$) and had a directionally
649 concordant beta estimate with the SOMAscan estimate.

650

651 **Candidate gene annotation**

652 We defined a pQTL as *cis* when the most significantly associated variant in the region was
653 located within 1Mb of the transcription start site (TSS) of the gene(s) encoding the protein.
654 pQTLs lying outside of the region were defined as *trans*. When considering the distance of the
655 lead *cis*-associated variant from the relevant TSS, only proteins that map to single genes on the
656 primary assembly in Ensembl v83 were considered.

657

658 For *trans* pQTLs, we sought to prioritise candidate genes in the region that might underpin the
659 genotype-protein association. We applied the ProGeM framework²⁶ that leverages a
660 combination of databases of molecular pathways, protein-protein interaction networks, and
661 variant annotation, as well as functional genomic data including eQTL and chromosome
662 conformation capture. In addition to reporting the nearest gene to the sentinel variant, ProGeM
663 employs complementary ‘bottom up’ and ‘top down’ approaches, starting from the variant and

664 protein respectively. For the ‘bottom up’ approach, the sentinel variant and corresponding
665 proxies ($r^2>0.8$) for each *trans* pQTL were first annotated using Ensembl VEP v83 (using the
666 ‘pick’ option) to determine whether variants were (1) protein-altering coding variants; (2)
667 synonymous coding or 5’/3’ untranslated region (UTR); (3) intronic or up/downstream; or (4)
668 intergenic. Second, we queried all sentinel variants and proxies against significant *cis* eQTL
669 variants (defined by beta distribution-adjusted empirical *p*-values using an FDR threshold of
670 0.05, see <http://www.gtexportal.org/home/documentationPage> for details) in any cell type or
671 tissue from the Genotype-Tissue Expression (GTEx) project v6³²
672 (<http://www.gtexportal.org/home/datasets>). Third, we also queried promoter capture Hi-C data
673 in 17 human primary hematopoietic cell types⁶¹ to identify contacts (with a CHICAGO score
674 >5 in at least one cell type) involving chromosomal regions containing a sentinel variant. We
675 considered gene promoters annotated on either fragment (i.e., the fragment containing the
676 sentinel variant or the other corresponding fragment) as potential candidate genes. Using these
677 three sources of information, we generated a list of candidate genes for the *trans* pQTLs. A
678 gene was considered a candidate if it fulfilled at least one of the following criteria: (1) it was
679 proximal (intragenic or ± 5 Kb from the gene) or nearest to the sentinel variant; (2) it contained
680 a sentinel or proxy variant ($r^2>0.8$) that was protein-altering; (3) it had a significant *cis* eQTL
681 in at least one GTEx tissue overlapping with a sentinel pQTL variant (or proxy); or (4) it was
682 regulated by a promoter annotated on either fragment of a chromosomal contact⁶¹ involving a
683 sentinel variant.

684

685 For the ‘top down’ approach, we first identified all genes with a TSS located within the
686 corresponding pQTL region using the GenomicRanges Bioconductor package⁶² with
687 annotation from a GRCh37 GTF file from Ensembl
688 (ftp://ftp.ensembl.org/pub/grch37/update/gtf/homo_sapiens/); file:

689 ‘Homo_sapiens.GRCh37.82.gtf.gz’, downloaded June 2016). We then identified any local
690 genes that had previously been linked with the corresponding *trans*-associated protein(s)
691 according to the following open source databases: (1) the Online Mendelian Inheritance in Man
692 (OMIM) catalogue⁶³ (<http://www.omim.org/>); (2) the Kyoto Encyclopedia of Genes and
693 Genomes (KEGG)⁶⁴ (<http://www.genome.jp/kegg/>); and (3) STRINGdb⁶⁵ ([http://string-
db.org/](http://string-
694 db.org/); v10.0). We accessed OMIM data via HumanMine web tool⁶⁶
695 (<http://www.humanmine.org/>; accessed June 2016), whereby we extracted all OMIM IDs for
696 (i) our *trans*-affected proteins and (ii) genes local ($\pm 500\text{Kb}$) to the corresponding *trans*-acting
697 variant. We extracted all human KEGG pathway IDs using the KEGGREST Bioconductor
698 package (<https://bioconductor.org/packages/release/bioc/html/KEGGREST.html>). In cases
699 where a *trans*-associated protein shared either an OMIM ID or a KEGG pathway ID with a
700 gene local to the corresponding *trans*-acting variant, we took this as evidence of a potential
701 functional involvement of that gene. We interrogated protein-protein interaction data by
702 accessing STRINGdb data using the STRINGdb Bioconductor package⁶⁷, whereby we
703 extracted all pairwise interaction scores for each *trans*-affected protein and all proteins with
704 genes local to the corresponding *trans*-acting variants. We took the default interaction score of
705 400 as evidence of an interaction between the proteins, therefore indicating a possible
706 functional involvement for the local gene. In addition to using data from open source databases
707 in our top down approach we also adopted a “guilt-by-association” (GbA) approach utilising
708 the same plasma proteomic data used to identify our pQTLs. We first generated a matrix
709 containing all possible pairwise Pearson’s correlation coefficients between our 3,283
710 SOMAmers. We then extracted the coefficients relating to our *trans*-associated proteins and
711 any proteins encoded by genes local to their corresponding *trans*-acting variants (where
712 available). Where the correlation coefficient was ≥ 0.5 we prioritised the relevant local genes
713 as being potential mediators of the *trans* signal(s) at that locus.

714

715 We report the potential candidate genes for our *trans* pQTLs from both the ‘bottom up’ and
716 ‘top down’ approaches, highlighting cases where the same gene was highlighted by both
717 approaches.

718

719 **Functional annotation of pQTLs**

720 Functional annotation of variants was performed using Ensembl VEP v83 using the ‘pick’
721 option. We tested the enrichment of significant pQTL variants for certain functional classes by
722 comparing to permuted sets of variants showing no significant association with any protein
723 ($p > 0.0001$ for all proteins tested). First, the regional sentinel variants were LD-pruned at r^2 of
724 0.1. Each time the sentinel variants were LD-pruned, one of the pairs of correlated variants was
725 removed at random and for each set of LD-pruned sentinel variants, 100 sets of equally sized
726 null permuted variants were sampled matching for MAF (bins of 5%), distance to TSS (bins of
727 0-0.5Kb, 0.5-2Kb, 2-5Kb, 5-10Kb, 10-20Kb, 20-100Kb and >100Kb in each direction) and LD
728 (\pm half the number of variants in LD with the sentinel variant at r^2 of 0.8). This procedure was
729 repeated 100 times resulting in 10,000 permuted sets of variants. An empirical p -value was
730 calculated as the proportion of permuted variant sets where the proportion that is classified as
731 a particular functional group exceeded that of the test set of sentinel pQTL variants, and we
732 used a significance threshold of $p = 0.005$ (0.05/10 functional classes tested).

733

734 **Evidence against aptamer-binding effects at *cis* pQTLs**

735 All protein assays that rely on binding (e.g., of antibodies or SOMAmers) are susceptible to
736 the possibility of binding-affinity effects, where protein-altering variants (PAVs) (or their
737 proxies in LD) are associated with protein measurements due to differential binding rather than
738 differences in protein abundance. To account for this potential effect, we performed conditional

739 analysis at all *cis* pQTLs where the sentinel variant was in LD ($r^2 \geq 0.1$ and $r^2 \leq 0.9$) with a PAV
740 in the gene(s) encoding the associated protein. First, variants were annotated with Ensembl
741 VEP v83 using the “per-gene” option. Variant annotations were considered protein-altering if
742 they were annotated as coding sequence variant, frameshift variant, in-frame deletion, in-frame
743 insertion, missense variant, protein altering variant, splice acceptor variant, splice donor
744 variant, splice region variant, start lost, stop gained, or stop lost. To avoid multi-collinearity,
745 PAVs were LD-pruned ($r^2 > 0.9$) using PLINK v1.9 before including them as covariates in the
746 conditional analysis on the meta-analysis summary statistics using GCTA v1.25.2. Coverage
747 of known common (MAF > 5%) PAVs in our data was checked by comparison with exome
748 sequences from ~60,000 individuals in the Exome Aggregation Consortium (ExAC
749 [<http://exac.broadinstitute.org>], downloaded June 2016).

750

751 **Testing for regulatory and functional enrichment**

752 We tested whether our pQTLs were enriched for functional and regulatory characteristics using
753 GARFIELD v1.2.0⁶⁹. GARFIELD is a non-parametric permutation-based enrichment method
754 that compares input variants to permuted sets matched for number of proxies ($r^2 \geq 0.8$), MAF
755 and distance to the closest TSS. It first applies “greedy pruning” ($r^2 < 0.1$) within a 1Mb region
756 of the most significant variant. GARFIELD annotates variants with more than a thousand
757 features, drawn predominantly from the GENCODE, ENCODE and ROADMAP projects,
758 which includes genic annotations, histone modifications, chromatin states and other regulatory
759 features across a wide range of tissues and cell types.

760

761 The enrichment analysis was run using all variants that passed our Bonferroni-adjusted
762 significance threshold ($p < 1.5 \times 10^{-11}$) for association with any protein. For each of the matching
763 criteria (MAF, distance to TSS, number of LD proxies), we used five bins. In total we tested

764 25 combinations of features (classified as transcription factor binding sites, FAIRE-seq,
765 chromatin states, histone modifications, footprints, hotspots, or peaks) with up to 190 cell types
766 from 57 tissues, leading to 998 tests. Hence, we considered enrichment with a $p < 5 \times 10^{-5}$
767 (0.05/998) to be statistically significant.

768

769 **Disease annotation**

770 To identify diseases that our pQTLs have been associated with, we queried our sentinel variants
771 and their strong proxies ($r^2 \geq 0.8$) against publicly available disease GWAS data using
772 PhenoScanner⁷⁰. A list of datasets queried is available at
773 <http://www.phenoscanter.medschl.cam.ac.uk/information.html>. For disease GWAS, results
774 were filtered to $p < 5 \times 10^{-8}$ and then manually curated to retain only the entry with the strongest
775 evidence for association (i.e. smallest p -value) per disease. Non-disease phenotypes such as
776 anthropometric traits, intermediate biomarkers and lipids were excluded manually.

777

778 ***Cis* eQTL overlap and enrichment of *cis* pQTLs for *cis* eQTLs**

779 For each regional sentinel *cis* pQTL variant, its strong proxies ($r^2 \geq 0.8$) were queried against
780 publicly available eQTL association data using PhenoScanner. *Cis* eQTL results were filtered
781 to retain only variants with $p < 1.5 \times 10^{-11}$. Only *cis* eQTLs for the same gene as the *cis* pQTL
782 protein were retained. We tested whether *cis* pQTLs were significantly enriched for eQTLs for
783 the corresponding gene compared to null sets of variants appropriately matched for MAF and
784 distance to nearest TSS. For this analysis, we restricted eQTL data to the GTEx project v6,
785 since this project provided complete summary statistics across a wide range of tissues and cell-
786 types, in contrast to many other studies which only report p -values below some significance
787 level. GTEx results were filtered to contain only variants lying in *cis* (i.e., within 1Mb) of genes
788 that encode proteins analysed in our study and only variants in both datasets were utilised.

789 For the enrichment analysis, the *cis* pQTL sentinel variants were first LD-pruned ($r^2 < 0.1$) and
790 the proportion of sentinel *cis* pQTL variants that are also eQTLs (at our pQTL significance
791 threshold [$p < 1.5 \times 10^{-11}$], conventional genomewide significance [$p < 5 \times 10^{-8}$] or a nominal *p*-
792 value threshold [$p < 1 \times 10^{-5}$]) for the same protein/gene was compared to a permuted set of
793 variants that were not pQTLs ($p > 0.0001$ for all proteins). We generated 10,000 permuted sets
794 of null variants for each significance threshold matched for MAF, distance to TSS and LD (as
795 described for functional annotation enrichment in **Functional annotation of pQTLs**). An
796 empirical *p*-value was calculated as the proportion of permuted variant sets where the
797 proportion that are also *cis* eQTLs exceeded that of the test set of sentinel *cis* pQTL variants.
798 At a stringent eQTL significance threshold ($p < 1.5 \times 10^{-11}$), we found significant enrichment of
799 *cis* pQTLs for eQTLs ($p < 0.0001$) (Supplementary Table 11) with 19.5% overlap observed
800 compared to a mean overlap of 1.8% in the null sets. Results were similar in sensitivity analyses
801 using the standard genome-wide or nominal significance thresholds as well as when using only
802 the sentinel variants at *cis* pQTLs that were robust to adjusting for PAVs (Supplementary Table
803 7), suggesting our results are robust to the choice of threshold and potential differential binding
804 effects.

805

806 **Colocalisation analysis**

807 Colocalisation testing was performed using the coloc package⁷¹. For testing colocalisation of
808 pQTLs and disease association signals, colocalisation testing was necessarily limited to disease
809 traits where full GWAS summary statistics had been made available. We obtained GWAS
810 summary statistics obtained through PhenoScanner. For testing colocalisation of pQTLs with
811 eQTLs, we used publically available summary statistics for expression traits from GTEx³². We
812 used the default priors. Regions for testing were determined by dividing the genome into 0.1cM
813 chunks using recombination data. Evidence for colocalisation was assessed using the posterior

814 probability (PP) for hypothesis 4 (that there is an association signal for both traits and they are
815 driven by the same causal variant[s]). Signals with $PP_4 > 0.5$ were deemed likely to colocalise
816 as this gives hypothesis 4 the highest likelihood of being correct, while $PP_4 > 0.8$ was deemed
817 to be ‘highly likely to colocalise’.

818

819 **Selection of genetic instruments for Mendelian randomisation**

820 In Mendelian randomisation (MR), genetic variants are used as ‘instrumental variables’ (IV)
821 for assessing the causal effect of the exposure (here a plasma protein) on the outcome (here
822 disease)^{10,72} (Extended Data Figure 6).

823

824 **Proteins in the *IL1RL1-IL18R1* locus and atopic dermatitis**

825 To identify the likely causal proteins that underpin the previous genetic association of the
826 *IL1RL1-IL18R1* locus (chr11:102.5-103.5Mb) with atopic dermatitis (AD)³⁵, we used the
827 following approach. For each protein encoded by a gene in the *IL1RL1-IL18R1* locus, we took
828 genetic variants that had a *cis* association at $p < 1 \times 10^{-4}$ and ‘LD-pruned’ them at $r^2 < 0.1$ to leave
829 largely independent variants. We then used these genetic variants to construct a genetic score
830 for each protein. Formally, we used these variants as instrumental variables for their respective
831 proteins in univariable MR. For multivariable MR, association estimates for all proteins in the
832 locus were extracted for all instruments. We used PhenoScanner to obtain association statistics
833 for the selected variants in the European-ancestry population of a recent large-scale GWAS
834 meta-analysis³⁵. Where the relevant variant was not available, the strongest proxy with $r^2 \geq 0.8$
835 was used.

836

837 **MMP-12 and coronary heart disease (CHD)**

838 To test whether plasma MMP-12 levels have a causal effect on risk of CHD, we selected
839 genetic variants in the *MMP12* gene region to use as instrumental variables. We constructed a
840 genetic score comprising 17 variants that had a *cis* association with MMP-12 levels at $p < 5 \times 10^{-8}$
841 ⁸ and that were not highly correlated with one another ($r^2 < 0.2$). To perform multivariable MR,
842 we used association estimates for these variants with other MMP proteins in the locus (MMP-
843 1, MMP-7, MMP-8, MMP-10, MMP-13). Summary associations for variants in the score with
844 CHD were obtained through PhenoScanner from a recent large-scale GWAS meta-analysis
845 which consists mostly (77%) individuals of European ancestry⁷³.

846

847 **MR analysis**

848 Two-sample univariable MR was performed for each protein separately using summary
849 statistics in the inverse-variance weighted method adapted to account for correlated variants⁷⁴⁻
850 ⁷⁵. For each of G genetic variants ($g = 1, \dots, G$) having per-allele estimate of the association
851 with the protein β_{Xg} and standard error σ_{Xg} , and per-allele estimate of the association with the
852 outcome (here, AD or CHD) β_{Yg} and standard error σ_{Yg} , the IV estimate ($\hat{\theta}_{XY}$) is obtained from
853 generalised weighted linear regression of the genetic associations with the outcome (β_Y) on the
854 genetic associations with the protein (β_X) weighting for the precisions of the genetic
855 associations with the outcome and accounting for correlations between the variants according
856 to the regression model:

857

$$858 \quad \beta_Y = \theta_{XY} \beta_X + \varepsilon, \quad \varepsilon \sim N(0, \Omega)$$

859

860 where β_Y and β_X are vectors of the univariable (marginal) genetic associations, and the
861 weighting matrix Ω has terms $\Omega_{g_1g_2} = \sigma_{Yg_1} \sigma_{Yg_2} \rho_{g_1g_2}$, and $\rho_{g_1g_2}$ is the correlation between
862 the g_1 th and g_2 th variants.

863

864 The IV estimate from this method is:

865

$$866 \quad \hat{\theta}_{XY} = (\beta_X^T \Omega^{-1} \beta_X)^{-1} \beta_X^T \Omega^{-1} \beta_Y$$

867

868 and the standard error is:

869

$$870 \quad \text{se}(\hat{\theta}_{XY}) = \sqrt{(\beta_X^T \Omega^{-1} \beta_X)^{-1}}$$

871

872 where T is a matrix transpose. This is the estimate and standard error from the regression model
873 fixing the residual standard error to 1 (equivalent to a fixed-effects model in a meta-analysis).

874

875 Genetic variants in univariable MR need to satisfy three key assumptions to be valid
876 instruments:

- 877 (1) the variant is associated with the risk factor of interest (i.e., the protein level),
- 878 (2) the variant is not associated with any confounder of the risk factor-outcome association,
- 879 (3) the variant is conditionally independent of the outcome given the risk factor and
880 confounders.

881

882 To account for potential effects of functional pleiotropy⁷⁶, we performed multivariable MR
883 using the weighted regression-based method proposed by Burgess *et al*⁷⁷. For each of K risk
884 factors in the model ($k = 1, \dots, K$), the weighted regression-based method is performed by
885 multivariable generalized weighted linear regression of the association estimates β_Y on each of
886 the association estimates with each risk factor β_{Xk} in a single regression model:

887

888
$$\beta_Y = \theta_{XY1} \beta_{X1} + \theta_{XY2} \beta_{X2} + \dots + \theta_{XYK} \beta_{XK} + \varepsilon, \quad \varepsilon \sim N(0, \Omega)$$

889

890 where β_{X1} is the vectors of the univariable genetic associations with risk factor 1, and so on.

891 This regression model is implemented by first pre-multiplying the association vectors by the

892 Cholesky decomposition of the weighting matrix, and then applying standard linear regression

893 to the transformed vectors. Estimates and standard errors are obtained fixing the residual

894 standard error to be 1 as above.

895

896 The multivariable MR analysis allows the estimation of the causal effect of a protein on disease

897 outcome accounting for the fact that genetic variants may be associated with multiple proteins

898 in the region. Causal estimates from multivariable MR represent direct causal effects,

899 representing the effect of intervening on one risk factor in the model while keeping others

900 constant.

901

902 **MMP-12 genetic score sensitivity analyses**

903 We performed two sensitivity analyses to determine the robustness of the MR findings. First,

904 we measured plasma MMP-12 levels using a different method (proximity extension assay;

905 Olink Bioscience, Uppsala, Sweden⁴) in 4,998 individuals, and used this to derive genotype-

906 MMP12 effect estimates for the 17 variants in our genetic score. Second, we obtained effect

907 estimates from a pQTL study based on SOMAscan assay measurements in an independent

908 sample of ~1,000 individuals²². In both cases the genetic score reflecting higher plasma MMP-

909 12 was associated with lower risk of CHD.

910

911 **Overlap of pQTLs with drug targets**

912 We used the Informa Pharmaprojects database from Citeline to obtain information on drugs
913 that target proteins assayed on the SOMAscan platform. This is a manually curated database
914 that maintains profiles for >60,000 drugs. For our analysis, we focused on the following
915 information for each drug: protein target, indications, and development status. We included
916 drugs across the development pipeline, including those in pre-clinical studies or with no
917 development reported, drugs in clinical trials (all phases), and launched/registered drugs. For
918 each protein assayed, we identified all drugs in the Informa Pharmaprojects with a matching
919 protein target based on UniProt ID. When multiple drugs targeted the same protein, we selected
920 the drug with the latest stage of development.

921

922 For drug targets with significant pQTLs, we identified the subset where the sentinel variant or
923 proxy variants in LD ($r^2 > 0.8$) are also associated with disease risk through PhenoScanner. We
924 used an internal Merck auto-encoding method to map GWAS traits and drug indications to a
925 common set of terms from the Medical Dictionary for Regulatory Activities (MedDRA).
926 MedDRA terms are organised into a hierarchy with five levels. We mapped each GWAS trait
927 and indication onto the ‘Lowest Level Terms’ (i.e. the most specific terms available). All
928 matching terms were recorded for each trait or indication. We matched GWAS traits to drug
929 indications based on the highest level of the hierarchy, called ‘System Organ Class’ (SOC).
930 We designated a protein as ‘matching’ if at least one GWAS trait term matched with at least
931 one indication term for at least one drug.

932

933 **Data availability**

934 Participant-level genotype and protein data, and full summary association results from the
935 genetic analysis, are available through the European Genotype Archive (accession number

936 EGAS00001002555). Summary association results will also be made available via FTP and
937 through PhenoScanner (<http://www.phenoscanter.medschl.cam.ac.uk>).

938 Online References

- 939 46. Di Angelantonio, E. *et al.* Efficiency and safety of varying the frequency of whole
940 blood donation (INTERVAL): a randomised trial of 45 000 donors. *Lancet* **390**, 2360-2371
941 (2017).
- 942 47. Moore, C. *et al.* The INTERVAL trial to determine whether intervals between blood
943 donations can be safely and acceptably decreased to optimise blood supply: study protocol for
944 a randomised controlled trial. *Trials* **15**, 363 (2014).
- 945 48. Gold, L. *et al.* Aptamer-based multiplexed proteomic technology for biomarker
946 discovery. *PLoS One* **5**, e15004 (2010).
- 947 49. Menni, C. *et al.* Circulating proteomic signatures of chronological age. *J Gerontol A*
948 *Biol Sci Med Sci* **70**, 809-16 (2014).
- 949 50. Sattlecker, M. *et al.* Alzheimer's disease biomarker discovery using SOMAscan
950 multiplexed protein technology. *Alzheimer's Dement.* **10**, 724–734 (2014).
- 951 51. McLaren, W. *et al.* Deriving the consequences of genomic variants with the Ensembl
952 API and SNP Effect Predictor. *Bioinformatics* **26**, 2069–70 (2010).
- 953 52. UniProt Consortium. UniProt: a hub for protein information. *Nucleic Acids Res.* **43**,
954 D204–D212 (2015).
- 955 53. Ashburner, M. *et al.* Gene Ontology: tool for the unification of biology. *Nat. Genet.* **25**,
956 25–29 (2000).
- 957 54. Ngo, D. *et al.* Aptamer-based proteomic profiling reveals novel candidate biomarkers
958 and pathways in cardiovascular disease. *Circulation* **134**, 270-285 (2016).
- 959 55. Chang, C. C. *et al.* Second-generation PLINK: rising to the challenge of larger and
960 richer datasets. *Gigascience* **4**, 7 (2015).
- 961 56. Marchini, J., Howie, B., Myers, S., McVean, G. & Donnelly, P. A new multipoint
962 method for genome-wide association studies by imputation of genotypes. *Nat. Genet.* **39**, 906–
963 913 (2007).
- 964 57. Willer, C. J., Li, Y. & Abecasis, G. R. METAL: fast and efficient meta-analysis of
965 genomewide association scans. *Bioinformatics* **26**, 2190–1 (2010).
- 966 58. Yang, J. *et al.* Conditional and joint multiple-SNP analysis of GWAS summary
967 statistics identifies additional variants influencing complex traits. *Nat. Genet.* **44**, 369–75, S1-
968 3 (2012).
- 969 59. Welter, D. *et al.* The NHGRI GWAS Catalog, a curated resource of SNP-trait
970 associations. *Nucleic Acids Res.* **42**, D1001-6 (2014).
- 971 60. Malone, J. *et al.* Modeling sample variables with an Experimental Factor Ontology.
972 *Bioinformatics* **26**, 1112–1118 (2010).

- 973 61. Javierre, B. M. *et al.* Lineage-specific genome architecture links enhancers and non-
974 coding disease variants to target gene promoters. *Cell* **167**, 1369–1384. e19 (2016).
- 975 62. Lawrence, M. *et al.* Software for computing and annotating genomic ranges. *PLoS*
976 *Comput. Biol.* **9**, e1003118 (2013).
- 977 63. Amberger, J. S., Bocchini, C. A., Schiettecatte, F., Scott, A. F. & Hamosh, A.
978 OMIM.org: Online Mendelian Inheritance in Man (OMIM(R)), an online catalog of human
979 genes and genetic disorders. *Nucleic Acids Res.* **43**, D789–D798 (2015).
- 980 64. Kanehisa, M., Sato, Y., Kawashima, M., Furumichi, M. & Tanabe, M. KEGG as a
981 reference resource for gene and protein annotation. *Nucleic Acids Res.* **44**, D457–D462 (2016).
- 982 65. Szklarczyk, D. *et al.* STRING v10: protein-protein interaction networks, integrated
983 over the tree of life. *Nucleic Acids Res.* **43**, D447–D452 (2015).
- 984 66. Smith, R. N. *et al.* InterMine: a flexible data warehouse system for the integration and
985 analysis of heterogeneous biological data. *Bioinformatics* **28**, 3163–3165 (2012).
- 986 67. Franceschini, A. *et al.* STRING v9.1: protein-protein interaction networks, with
987 increased coverage and integration. *Nucleic Acids Res.* **41**, D808–D815 (2013).
- 988 68. Lek, M. *et al.* Analysis of protein-coding genetic variation in 60,706 humans. *Nature*
989 **536**, 285–291 (2016).
- 990 69. Iotchkova, V. *et al.* GARFIELD - GWAS Analysis of Regulatory or Functional
991 Information Enrichment with LD correction. *bioRxiv* (2016). doi:10.1101/085738
- 992 70. Staley, J. R. *et al.* PhenoScanner: a database of human genotype-phenotype
993 associations. *Bioinformatics* **32**, 3207–3209 (2016).
- 994 71. Giambartolomei, C. *et al.* Bayesian test for colocalisation between pairs of genetic
995 association studies using summary statistics. *PLoS Genet.* **10**, e1004383 (2014).
- 996 72. Hingorani, A. & Humphries, S. Nature’s randomised trials. *Lancet* **366**, 1906–8 (2005).
- 997 73. Nikpay, M. *et al.* A comprehensive 1,000 Genomes-based genome-wide association
998 meta-analysis of coronary artery disease. *Nat. Genet.* **47**, 1121–30 (2015).
- 999 74. Burgess, S., Butterworth, A. & Thompson, S. G. Mendelian randomization analysis
1000 with multiple genetic variants using summarized data. *Genet. Epidemiol.* **37**, 658–665 (2013).
- 1001 75. Burgess, S., Dudbridge, F. & Thompson, S. G. Combining information on multiple
1002 instrumental variables in Mendelian randomization: comparison of allele score and
1003 summarized data methods. *Stat. Med.* **35**, 1880–906 (2016).
- 1004 76. Burgess, S. & Thompson, S. G. Multivariable Mendelian randomization: the use of
1005 pleiotropic genetic variants to estimate causal effects. *Am. J. Epidemiol.* **181**, 251–60 (2015).
- 1006 77. Burgess, S., Dudbridge, F. & Thompson, S. G. Re: ‘Multivariable Mendelian
1007 randomization: the use of pleiotropic genetic variants to estimate causal effects’. *Am. J.*
1008 *Epidemiol.* **181**, 290–1 (2015).

1009 78. Merkel, P. A. *et al.* Identification of functional and expression polymorphisms
1010 associated with risk for anti-neutrophil cytoplasmic autoantibody-associated vasculitis.
1011 *Arthritis Rheumatol.* **69**, 1054-1066 (2016).

1012

1013

1014 **Supplementary Information**

1015 Supplementary Information is available in the online version of the paper.

1016 **Acknowledgements**

1017 Aaron Day-Williams, Joshua McElwee, Dorothee Diogo, William Astle, Emanuele Di
1018 Angelantonio, Ewan Birney, Arianne Richard, Justin Mason and Michael Inouye commented
1019 helpfully on the manuscript; Mark Sharp helped with mapping drug indications to GWAS
1020 traits.

1021 We thank the following: participants in INTERVAL and its study co-ordination team (at the
1022 Universities of Cambridge and Oxford and at NHSBT), including the staff at 25 NHSBT blood
1023 donation centres; the INTERVAL Operations Team led by Dr Richard Houghton and Dr
1024 Carmel Moore; the INTERVAL Data Management Team led by Dr Matthew Walker; and staff
1025 at SomaLogic for processing and running the proteomic assays.

1026 The Cardiovascular Epidemiology Unit at the University of Cambridge is supported by the UK
1027 Medical Research Council (G0800270), British Heart Foundation (SP/09/002), UK National
1028 Institute for Health Research Cambridge Biomedical Research Centre, European Research
1029 Council (268834), and European Commission Framework Programme 7 (HEALTH-F2-2012-
1030 279233). B.B.S. was funded by the Cambridge School of Clinical Medicine MRC/Sackler Prize
1031 PhD Studentship (MR/K50127X/1) and supported by the Cambridge School of Clinical
1032 Medicine MB-PhD programme. J.E.P. was funded by a British Heart Foundation Clinical
1033 Research Fellowship through the BHF Cambridge Centre of Excellence [RE/13/6/30180] and
1034 a UK Research Innovation Clinician Scientist Fellowship (MR/S004068/1). P.S. was supported
1035 by a Rutherford Fund Fellowship (MR/S003746/1). D.S.P. and D.S. were funded by the
1036 Wellcome Trust (105602/Z/14/Z). N.S. was supported by the Wellcome Trust (WT098051 and
1037 WT091310), the EU FP7 (EPIGENESYS 257082 and BLUEPRINT HEALTH-F5-2011-
1038 282510). J.A.T was supported by the supported by the Wellcome Trust (091157) and JDRF (9-

1039 2011-253). K.S. was funded by the Biomedical Research Program funds at Weill Cornell
1040 Medicine in Qatar, a program funded by the Qatar Foundation. J.D. was supported by a British
1041 Heart Foundation Professor, European Research Council Senior Investigator, and National
1042 Institute for Health Research (NIHR) Senior Investigator. The INTERVAL study was funded
1043 by NHSBT (11-01-GEN) and has been supported by the NIHR-BTRU in Donor Health and
1044 Genomics (NIHR BTRU-2014-10024) at the University of Cambridge in partnership with
1045 NHSBT. This study was partially funded by Merck and Co., Kenilworth, NJ, USA. The views
1046 expressed are those of the authors and not necessarily those of the NHS, the NIHR, the
1047 Department of Health of England, or NHSBT.

1048

1049 **Author Contributions**

1050 Conceptualization and experimental design: J.D., A.S.B., B.B.S., H.R., R.M.P.; Methodology:
1051 B.B.S., A.B.S., J.C.M., J.E.P., H.R., S.B.; Analysis: B.B.S., J.C.M., J.E.P., D.S., J.B., J.R.S.,
1052 T.J., E.P., P.S., C.O-W., M.A.K., S.K.W., A.C., N.B., S.L.S.; Contributed reagents, materials,
1053 protocols or analysis tools: N.J., S.K.W., E.S.Z., J.B., M.A.K., J.R.S., B.P.P.; Supervision:
1054 A.S.B., H.R., J.D., R.M.P., C.S.F., D.S.P., A.M.W.; Writing - principal: B.B.S., A.S.B., J.E.P.,
1055 J.C.M., H.R., J.D.; Writing – review and editing: B.B.S., A.S.B., J.E.P., J.C.M., J.D., H.R.,
1056 K.S., A.M.W., N.J., D.J.R., J.A.T., D.S.P., N.S., C.S.F., R.M.P; Creation of the INTERVAL
1057 BioResource: J.R.B., D.J.R., W.H.O., N.W.M., J.D.; Funding acquisition: N.W.M., J.R.B.,
1058 D.J.R., W.H.O.,H.R., R.M.P., J.D.; all authors critically reviewed the manuscript.

1059

1060 **Author Information**

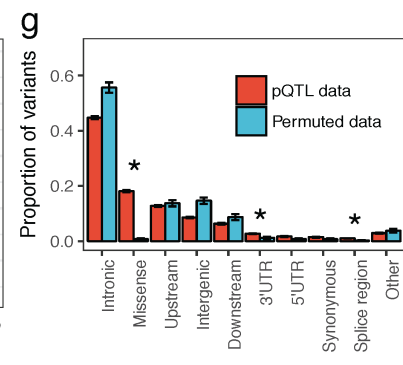
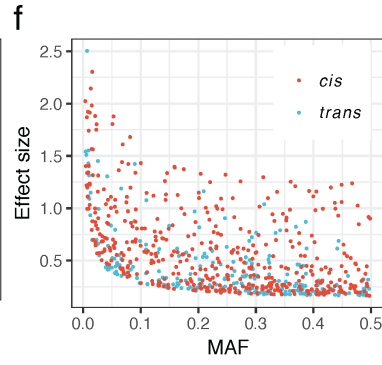
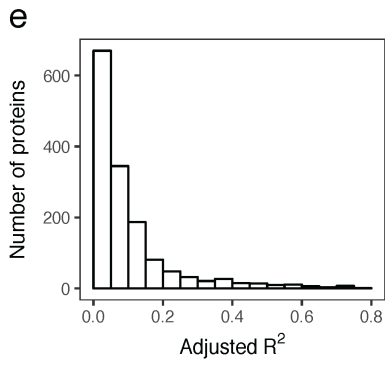
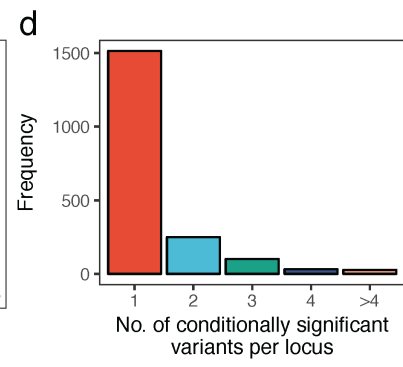
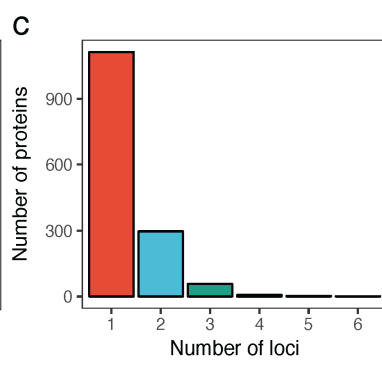
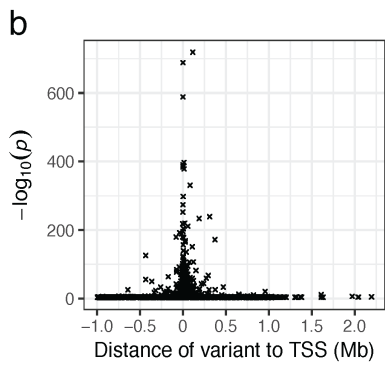
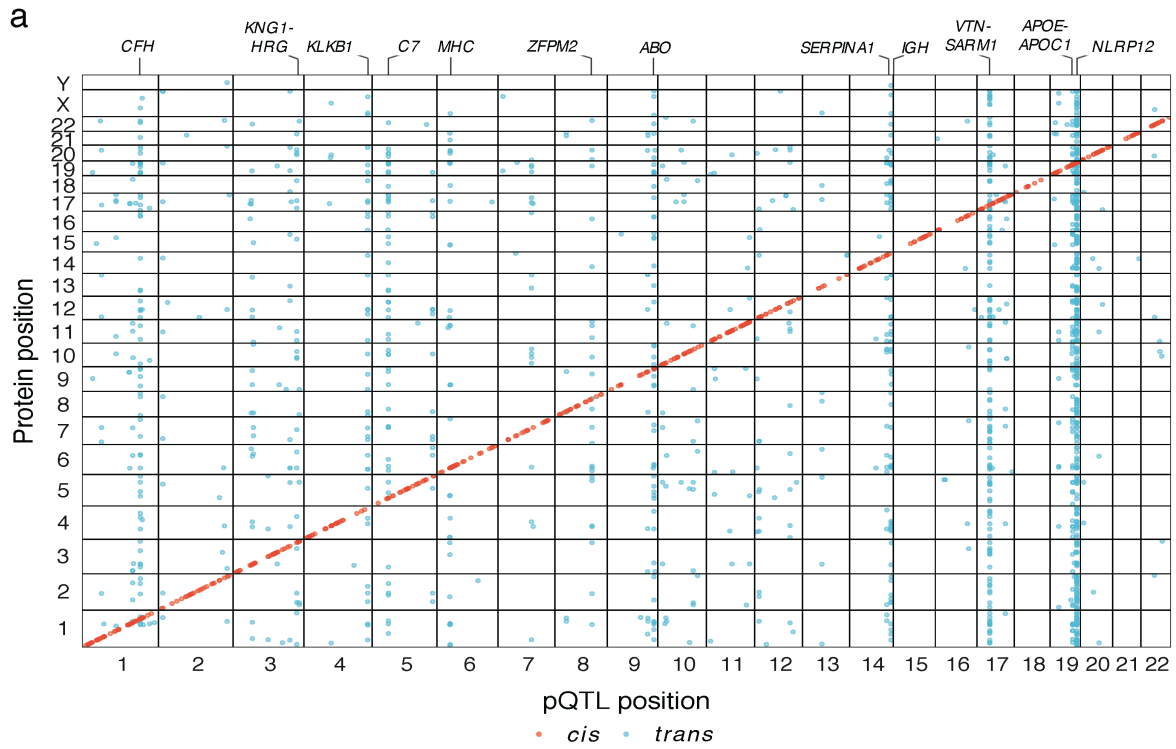
1061 Reprints and permissions information is available at www.nature.com/reprints. The authors
1062 declare the following competing financial interests: J.C.M., A.C., C.S.F., R.M.P., H.R. are

1063 employees at MRL, Merck & Co., Inc. S.K.W., E.S.Z., N.J. are employees and stakeholders in
1064 SomaLogic, Inc. The other authors have nothing to disclose. Correspondence and requests for
1065 materials should be addressed to A.S.B. (asb38@medschl.cam.ac.uk) and J.D.
1066 (jd292@medschl.cam.ac.uk).
1067

1068 **Figures**

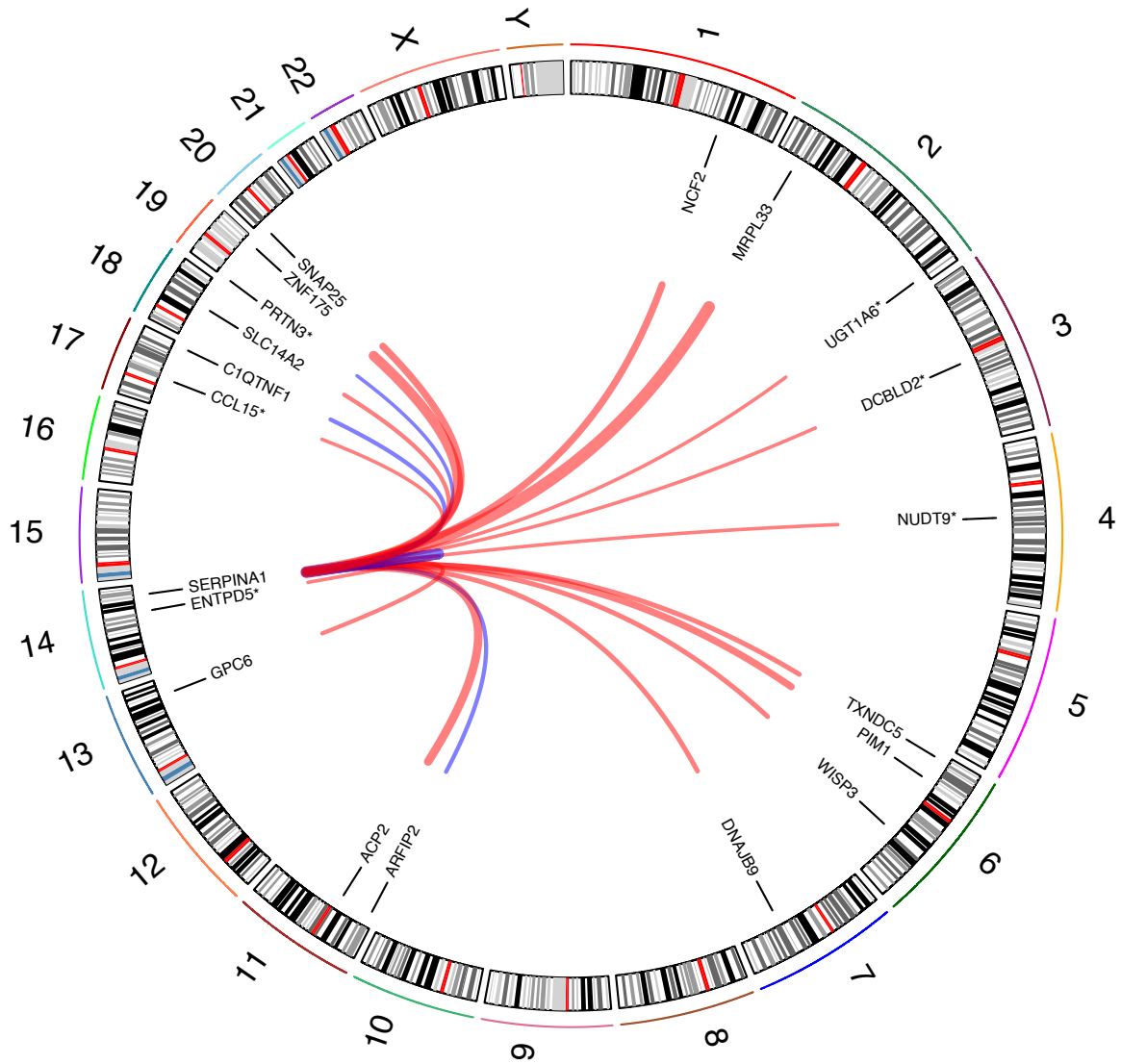
1069 **Figure 1. The genetic architecture of plasma protein levels.**

- 1070 (a) Genomic location of pQTLs. Plot of sentinel variants for pQTLs (red= *cis*, blue= *trans*). Y-
1071 axis indicates the position of the gene that encodes the associated protein. The 12 most
1072 associated regions of the genome are annotated.
- 1073 (b) Plot of the statistical significance of the most associated (sentinel) *cis* variant for each
1074 protein against the distance from the transcription start site (TSS).
- 1075 (c) Histogram of the number of significantly associated loci per protein.
- 1076 (d) Histogram of the number of conditionally significant signals within each associated locus.
- 1077 (e) Histogram of protein variance explained (adjusted R^2) by conditionally significant variants.
- 1078 (f) Distribution of effect-size against minor allele frequency (MAF) for *cis* and *trans* pQTLs.
- 1079 (g) Distribution of the predicted consequences of the sentinel pQTL variants compared to
1080 matched permuted null sets of variants. Asterisks highlight empirical enrichment $p < 0.005$.



1082 **Figure 2. Missense variant rs28929474 in *SERPINA1* is a *trans* pQTL hotspot.**

1083 Numbers (outermost) indicate chromosomes. Interconnecting lines link the genomic location
1084 of rs28929474 and the genes encoding significantly associated ($p < 1.5 \times 10^{-11}$) proteins. Line
1085 thickness is proportional to the effect-size of the associations with red positive and blue
1086 negative. Genes with an asterisk indicate *trans* pQTLs that reached conventional genome-wide
1087 significance ($p < 5 \times 10^{-8}$).
1088
1089

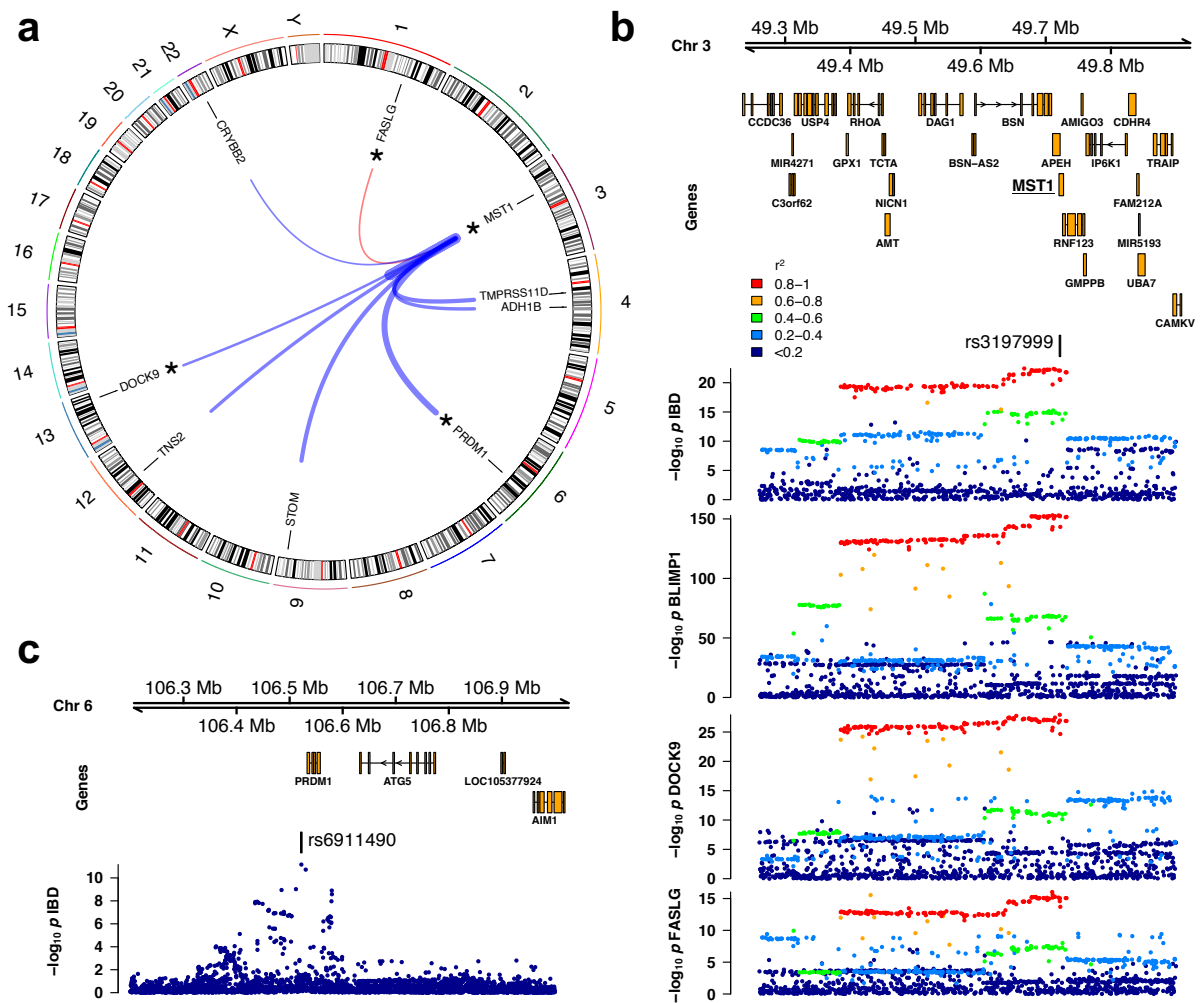


1090

1091
 1092
 1093
 1094
 1095
 1096
 1097
 1098
 1099
 1100
 1101
 1102
 1103
 1104

Figure 3. *Trans* pQTL for BLIMP1 at an inflammatory bowel disease (IBD) associated genetic variant in *MST1*.

(a) IBD-associated missense variant (rs3197999:A) in the *MST1* region on chromosome 3 is associated with abundance of multiple proteins in plasma. Interconnecting lines link the genomic location of rs3197999 and the genes encoding significantly associated ($p < 1.5 \times 10^{-11}$) proteins. Line thickness is proportional to the effect size. Red and blue lines indicate positive and negative effects of the IBD risk allele, respectively. * highlights genes in IBD GWAS loci. (b) Regional association plots of the IBD susceptibility locus at *MST1*, showing IBD association signal (top) and *trans* pQTLs for BLIMP1, DOCK9 and FASLG (bottom 3 panels). Colour key indicates r^2 with rs3197999. (c) Regional association plot of the IBD susceptibility locus on chromosome 6 adjacent to the *PRDM1* gene, which encodes BLIMP1. All IBD association data are for European participants from Liu *et al.*, 2015.



1105
 1106

1107 **Figure 4. *SERPINA1*, *PRTN3* and vasculitis.**

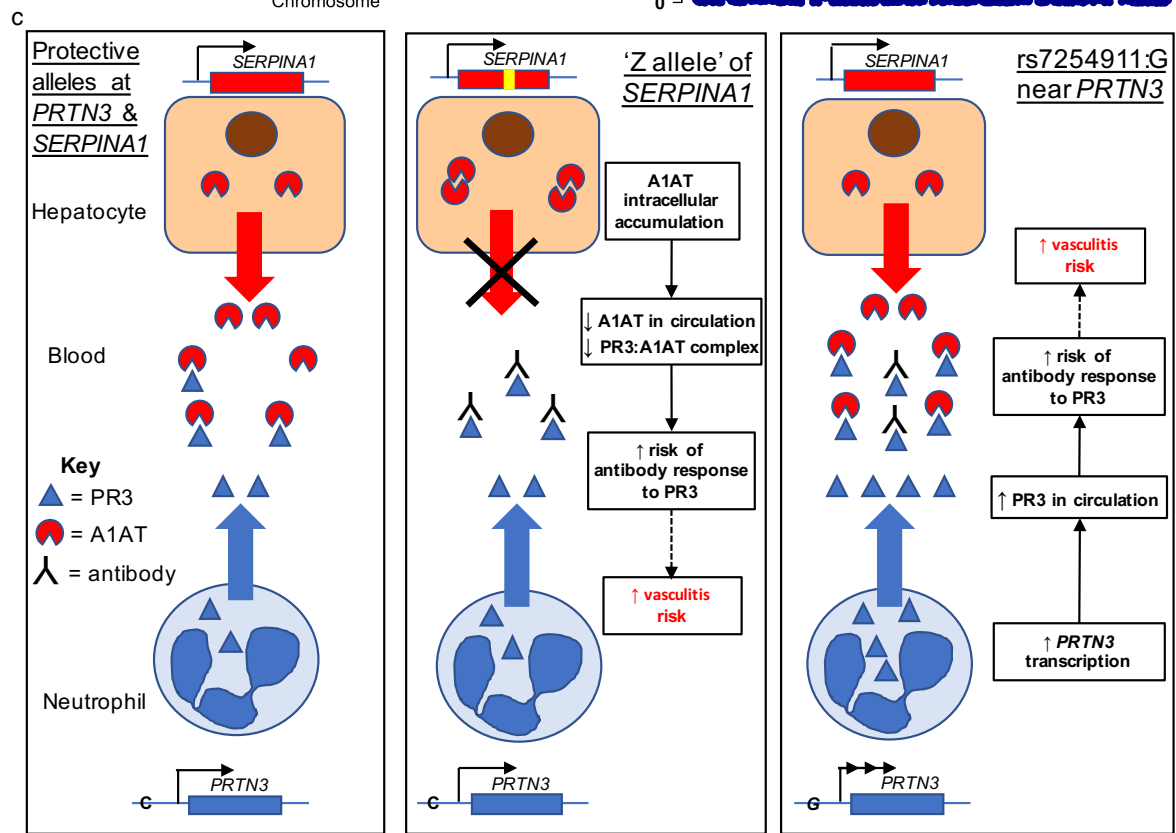
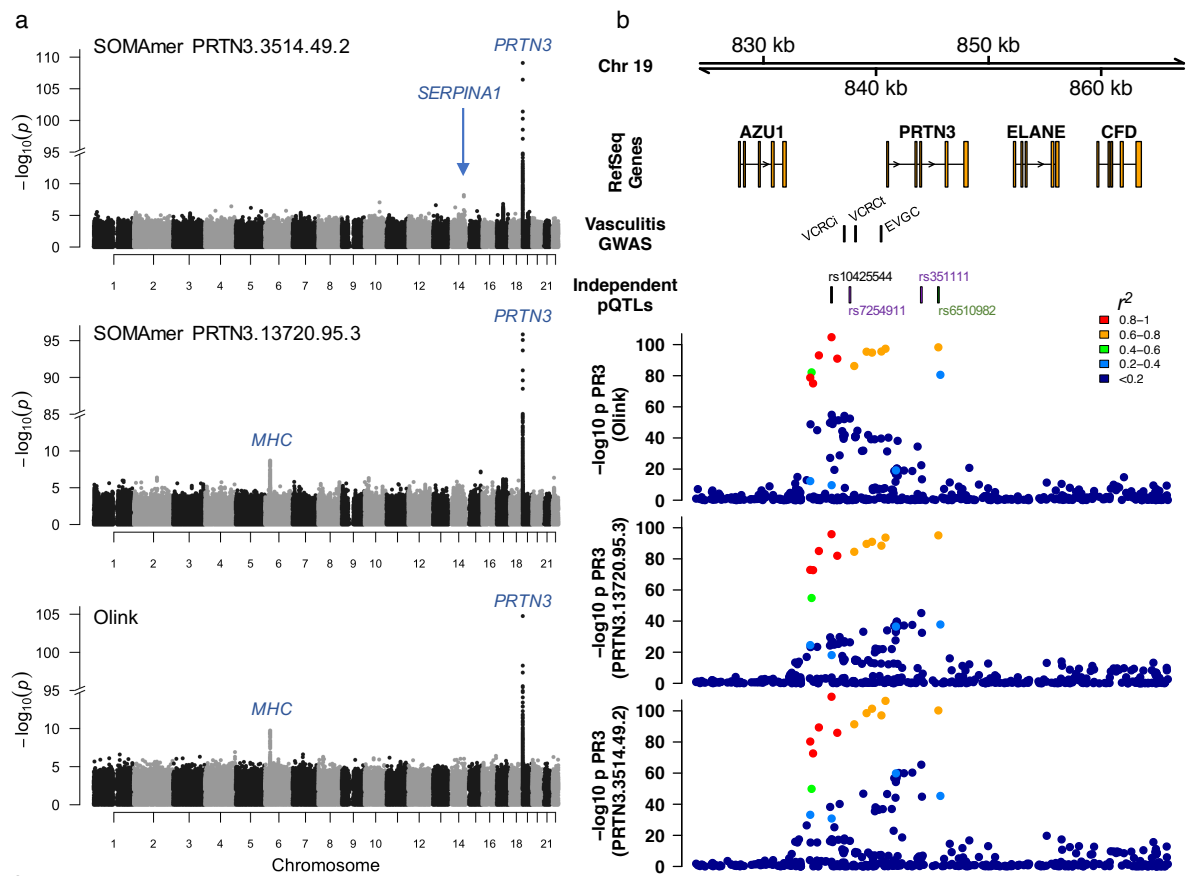
1108

1109 a) Manhattan plots for GWAS of plasma PR3 measured with the two SOMAmers and the Olink
1110 assay, showing the *cis* pQTL at *PRTN3* (which encodes PR3) for all three PR3 assays and the
1111 *SERPINA1 trans* pQTL for SOMAmer PRTN3.3514.49.2.

1112 b) Regional association plots at the *PRTN3* region for the two PR3 SOMAmers and the Olink
1113 PR3 assay. LD to the sentinel variant rs10425544 is indicated by the colour key. ‘Vasculitis
1114 GWAS’ track shows the variants reported in GWASs of ANCA-associated vasculitis. VCRCi=
1115 rs138303849, most significant imputed variant from the Vasculitis Clinical Research
1116 Consortium⁷⁸; VCRCt = rs62132293, directly genotyped SNP reported by the VCRC; EVGC=
1117 rs62132295, variant reported by the European Vasculitis Genetics Consortium³⁹ (see
1118 Supplementary Note). ‘Independent pQTL’ track indicates the position of conditionally
1119 independent PR3 pQTL variants (black lettering = lead variant for both SOMAmers; purple
1120 and green = conditionally independent variants for SOMAmer PRTN3.3514.49.2 and
1121 PRTN3.13720.95.3, respectively).

1122 c) Proposed mechanisms by which *PRTN3* and *SERPINA1* impact PR3 levels and therefore
1123 influence vasculitis risk. Left panel: individuals without either the *PRTN3* or the *SERPINA1*
1124 vasculitis risk alleles. Middle panel: in individuals with the *SERPINA1* Z-allele, A1AT
1125 polymerises and is accumulated intracellularly resulting in reduced secretion into the
1126 circulation. As a consequence of reduced circulating A1AT, plasma free PR3 is increased.
1127 Right panel: individuals with rs7254911:G, a *cis* pQTL upstream of *PRTN3*, have higher
1128 circulating levels of total PR3. Increases in either free or total PR3 predispose to loss of immune
1129 tolerance, with increased formation of anti-PR3 antibodies and risk of vasculitis.

1130



1131
1132

1133 **Figure 5. Evaluation of causal role of proteins in disease.**
1134 Forest plot of univariable and multivariable Mendelian randomization (MR) estimates. (a)
1135 Proteins in the *IL1RL1-IL18R1* locus and risk of atopic dermatitis (AD). No univariable MR
1136 estimates available for IL1R1 and IL18RAP due to no significant pQTLs to select as a “genetic
1137 instrument”. (b) MMP-12 levels and risk of coronary heart disease (CHD). Above: MR
1138 estimates. Below: estimated effects (with 95% confidence intervals) on plasma MMP-12 and
1139 CHD risk for each variant used in the genetic score.
1140

